THE ASTROPHYSICAL JOURNAL SUPPLEMENT SERIES, 134:151–171, 2001 May

PROTON-INDUCED THERMONUCLEAR REACTION RATES FOR $A = 20$–40 NUCLEI

CHRISTIAN ILIADIS
University of North Carolina at Chapel Hill, Chapel Hill, NC 27599-3255; and Triangle Universities Nuclear Laboratory, Durham, NC 27708-0308; iliadis@unc.edu

JOHN M. D'AURIA
Simon Fraser University, Burnaby, BC V5A 1S6, Canada; dauria@sfu.ca

SUMNER STARRFIELD
Arizona State University, Tempe, AZ 85287-1504; sumner.starrfield@asu.edu

WILLIAM J. THOMPSON
University of North Carolina at Chapel Hill, Chapel Hill, NC 27599-3255; wmjthompson@msn.com

AND

MICHAEL WIESCHER
University of Notre Dame, Notre Dame, IN 46616; wiescher.1@nd.edu
Received 2000 August 24; accepted 2000 December 6

ABSTRACT

Proton-induced reaction rates on 26 stable and 29 unstable target nuclei in the mass $A = 20$–40 region have been evaluated and compiled. Recommended reaction rates, assuming that all interacting nuclei are in the ground state, are presented in tabular form on a temperature grid in the range $T = 0.01$–10.0 GK. Most reaction rates involving stable targets were normalized to a set of measured standard resonance strengths in the sd shell. For the majority of reaction rates, experimental information from transfer reaction studies has been used consistently. Our results are compared with recent statistical model (Hauser-Feshbach) calculations. Reaction rate uncertainties are presented and amount to several orders of magnitude for many of the reactions. Several of these reaction rates and/or their corresponding uncertainties deviate from results of previous compilations. In most cases, the deviations are explained by the fact that new experimental information became available recently. Examples are given for calculating reaction rates and reverse reaction rates for thermally excited nuclei from the present results. The survey of literature for this review was concluded in 2000 August.

Subject headings: nuclear reactions, nucleosynthesis, abundances — stars: evolution

On-line material: machine-readable tables

1. INTRODUCTION

Thermonuclear reactions are the source of energy for various phenomena in the universe. At the same time, they change the composition of the nuclear fuel. Observables such as luminosity or elemental abundances represent signatures that need to be explained by appropriate astrophysical models. Therefore accurate model calculations require (among other input information) reliable estimates of thermonuclear reaction rates. The most widely used compilation of experimental thermonuclear reaction rates for low-mass target nuclei ($A = 1$–30) was published by Fowler and collaborators (Caughlan & Fowler 1988 and references therein). An updated compilation of experimental reaction rates involving a similar range of target nuclei ($A = 1$–28) was recently presented by Angulo et al. (1999).

The present work was originally motivated by our interest in various hydrogen-burning scenarios covering a large range of stellar temperatures, such as globular cluster red giants, novae, X-ray bursts, and supernovae. Moreover, observations of intermediate-mass elements with $A = 20$–40 in some of these sites could provide important constraints on the astrophysical models. Consequently, it is desirable to extend the set of compiled proton-induced reaction rates to mass $A = 40$. In addition, at elevated stellar temperatures a large number of short-lived target nuclei take part in hydrogen-burning nucleosynthesis. However, only a few reaction rates involving unstable targets were compiled by either Caughlan & Fowler (1988) or Angulo et al. (1999). Thus, it is also important to extend the set of compiled proton-induced reaction rates to short-lived nuclei.

In this paper, we present evaluated and compiled proton-induced reaction rates on stable and unstable target nuclei in the mass $A = 20$–40 region. For stable targets, our results can be regarded as an extension of previous work to the mass $A = 40$ range. Moreover, present and previous compilations overlap in the mass $A = 20$–30 range, and it is interesting to compare the results and discuss differences. For unstable targets, proton-induced reaction rates have been published previously (see, for example, Wallace & Woosley 1981; Wiescher et al. 1986; Van Wormer et al. 1994; Herndl et al. 1995). However, the present work represents the first systematic compilation involving unstable target nuclei in the mass range $A = 20$–40.

Thermonuclear rates based on the Hauser-Feshbach statistical model of nuclear reactions have been published by several research groups. For a recent compilation, see Rauscher & Thielemann (2000). These calculations are mainly based on *theory*. The results of the present work and of Angulo et al. (1999) are mainly based on *experimental data* and, consequently, are preferable to Hauser-Feshbach reaction rates in astrophysical model calculations. However, the statistical model calculations are important in the present work. First, at very high stellar temperatures, we have frequently adopted the results of Hauser-Feshbach calculations, normalized to our experimental reaction rates.

TABLE 1

RECOMMENDED ABSOLUTE RESONANCE STRENGTHS

E_R^{lab} [a] (keV)	J_R^{π} [a]	$\omega\gamma_{cm}^{standard}$ [b] (eV)	$\Delta\omega\gamma/\omega\gamma$ [c] (Percent)	Reference
^{23}Na$(p,\gamma)^{24}$Mg:				
512	$(1,2^+)$	$(9.13 \pm 1.25) \times 10^{-2}$	14	1
^{24}Mg$(p,\gamma)^{25}$Al:				
223	$1/2^+$	$(1.27 \pm 0.09) \times 10^{-2}$	7	3
419	$3/2^+$	$(4.16 \pm 0.26) \times 10^{-2}$	6	2
^{25}Mg$(p,\gamma)^{26}$Al:				
435	4^-	$(9.42 \pm 0.65) \times 10^{-2}$	7	2
591	1^+	$(2.28 \pm 0.17) \times 10^{-1}$	7	4
^{26}Mg$(p,\gamma)^{27}$Al:				
338	$3/2^-$	$(2.73 \pm 0.16) \times 10^{-1}$	6	2
454	$1/2^+$	$(7.15 \pm 0.41) \times 10^{-1}$	6	2
1966.....	$5/2^+$	$(5.15 \pm 0.45) \times 10^{0}$	9	1
^{27}Al$(p,\gamma)^{28}$Si:				
406	4^+	$(8.63 \pm 0.52) \times 10^{-3}$	6	2
632	3^-	$(2.64 \pm 0.16) \times 10^{-1}$	6	1
992	3^+	$(1.91 \pm 0.11) \times 10^{0}$	6	1
^{30}Si$(p,\gamma)^{31}$P:				
620	$1/2^-$	$(1.95 \pm 0.10) \times 10^{0}$	5	1
^{31}P$(p,\gamma)^{32}$S:				
642	1^-	$(5.75 \pm 0.50) \times 10^{-2}$	9	1
811	2^+	$(2.50 \pm 0.20) \times 10^{-1}$	8	1
^{34}S$(p,\gamma)^{35}$Cl:				
1211.....	$7/2^-$	$(4.50 \pm 0.50) \times 10^{0}$	11	1
^{35}Cl$(p,\gamma)^{36}$Ar:				
860	3^-	$(7.00 \pm 1.00) \times 10^{-1}$	14	1
^{36}Ar$(p,\gamma)^{37}$K:				
918	$5/2^+$	$(2.38 \pm 0.19) \times 10^{-1}$	8	5
^{37}Cl$(p,\gamma)^{38}$Ar:				
846	1^-	$(1.25 \pm 0.16) \times 10^{-1}$	13	1
^{39}K$(p,\gamma)^{40}$Ca:				
2042.....	1^+	$(1.79 \pm 0.19) \times 10^{0}$	11	1
^{40}Ca$(p,\gamma)^{41}$Sc:				
1842.....	$7/2^+$	$(1.40 \pm 0.15) \times 10^{-1}$	11	1

[a] Endt (1990, 1998).

[b] Resonance strength defined by equation (16).

[c] Resonance strength uncertainty (in percent).

REFERENCES.—(1) Paine & Sargood 1979; (2) Powell et al. 1998; (3) Powell et al. 1999; (4) Anderson et al. 1980; (5) Goosman & Kavanagh 1967 and Mohr et al. 1999, weighted average of values.

Second, several accurately known experimental reaction rates presented here have been used to test the reliability of current Hauser-Feshbach calculations involving sd shell target nuclei.

A review of the formalism to calculate thermonuclear reaction rates is given in § 2. In § 3, we explain our procedures in more detail. A standard set of absolute resonance strengths for sd shell nuclei that has been adopted in the present work is discussed in § 3.2. The systematic use of transfer reaction data to improve estimates of reaction rates is described in § 3.3. The comparison of our results and theoretical Hauser-Feshbach calculations is discussed in § 3.4. Reaction rates are presented in § 4. A summary and conclusions are presented in § 5. In Appendix A, we give examples of how to calculate reaction rates involving thermally excited nuclei and reverse reaction rates from the results presented here. Nuclear data for specific reactions are provided in Appendix B.

2. THERMONUCLEAR REACTION RATES

The total rate for a (p,γ) or (p,α) reaction in units of cm^3 s^{-1} mol^{-1} is given by

$$N_A\langle\sigma v\rangle = 3.7318 \times 10^{10}\mu^{-1/2}T_9^{-3/2} \times \int_0^{\infty}\sigma(E)Ee^{-11.605E/T_9}\,dE\,, \quad (1)$$

where E is the center-of-mass bombarding energy in megaelectron volts, T_9 is the temperature in gigakelvins, and μ is the reduced mass in amu (Fowler, Caughlan, & Zimmerman 1967). The total cross section σ (in barns) is determined by the sum of resonant and nonresonant contributions to the nuclear reaction mechanism.

2.1. *Nonresonant and Narrow-Resonance Reaction Rates*

The nonresonant cross section varies smoothly with bombarding proton energy E and is usually converted into the astrophysical S-factor, defined by

$$S(E) = \sigma(E)Ee^{2\pi\eta}\,, \quad (2)$$

where η denotes the Sommerfeld parameter. If the energy dependence of the S-factor is weak, substitution of equation (2) into equation (1) gives rise to an integrand whose energy dependence is determined by the penetrability through the Coulomb barrier and the Maxwell-Boltzmann energy distribution of the interacting nuclei. The so-called Gamow peak represents the bombarding energy range of effective stellar burning at a given temperature. If the S-factor can be approximated by a polynomial

$$S(E) = S(0) + ES'(0) + \tfrac{1}{2}E^2S''(0)\,, \quad (3)$$

then the nonresonant reaction rates are obtained by using the relations

$$N_A\langle\sigma v\rangle_{nr} = 4.339 \times 10^8\tau^2\,\frac{1}{\mu Z}\,e^{-\tau}S_{eff}\,, \quad (4)$$

$$\tau = 4.248\left(\frac{Z^2\mu}{T_9}\right)^{1/3}\,, \quad (5)$$

$$S_{eff} = S(0)\left[1 + \frac{5}{12\tau} + \frac{S'(0)}{S(0)}\left(E_0 + \frac{35}{36}\,kT\right) + \frac{1}{2}\,\frac{S''(0)}{S(0)}\left(E_0^2 + \frac{89}{36}\,E_0\,kT\right)\right](MeV\ b)\,, \quad (6)$$

where Z is the number of protons in the target nucleus and k is the Boltzmann constant (Fowler et al. 1967). The location E_0 and $1/e$ width Δ of the Gamow peak (in megaelectron volts) are given by

$$E_0 = 0.122(Z^2\mu T_9^2)^{1/3}\,, \quad (7)$$

$$\Delta = 0.237(Z^2\mu T_9^5)^{1/6}\,, \quad (8)$$

respectively.

The contribution of isolated and narrow resonances to the total reaction rate is given by

$$N_A\langle\sigma v\rangle_r = 1.540 \times 10^{11}(\mu T_9)^{-3/2}\sum_i \omega\gamma_i\,e^{-11.605E_{R_i}/T_9}\,, \quad (9)$$

where the E_{R_i} are the center-of-mass energies and the $\omega\gamma_i$ are the strengths of the resonances in megaelectron volts (Fowler et al. 1967). Equation (9) is derived from equation (1) by describing each resonance with a Breit-Wigner expression and by assuming that the energy dependences of

TABLE 2

INFORMATION ON REACTION RATES COMPILED IN THE PRESENT WORK

Reaction (1)	$Q_{p,\gamma}$ [a] (keV) (2)	Reference (3)	N_R (4)	$E^{cm}_{R,min} - E^{cm}_{R,max}$ (keV) (5)	$S_{DC}(0)$ (keV b) (6)
^{20}Ne$(p,\gamma)^{21}$Na	2431.3 ± 0.7	Angulo et al. 1999	8	366–2035	44.0
^{21}Ne$(p,\gamma)^{22}$Na	6739.4 ± 0.5	Present work	46	17–1937	20.0
^{22}Ne$(p,\gamma)^{23}$Na	8794.1 ± 0.2	Hale et al. 2001	55	28–1823	62.0
^{20}Na$(p,\gamma)^{21}$Mg	3222 ± 18	Kubono et al. 1992	6	28–794	2.6
^{21}Na$(p,\gamma)^{22}$Mg	5501.5 ± 1.5	Bateman et al. 2001	4	212–541	7.9
^{22}Na$(p,\gamma)^{23}$Mg	7579.5 ± 1.3	Angulo et al. 1999	21	3–1214	18.0[b]
^{23}Na$(p,\gamma)^{24}$Mg	11692.9 ± 0.2	Hale et al. 2001	57	2–2388	24.8
^{23}Na$(p,\alpha)^{20}$Ne	2376.5 ± 0.2	Hale et al. 2001	52	2–2328	...
^{22}Mg$(p,\gamma)^{23}$Al	123 ± 19	Caggiano et al. 2001	1	425	0.57
^{23}Mg$(p,\gamma)^{24}$Al	1871.3 ± 4.1	Herndl et al. 1998	4	478–1029	20.8
^{24}Mg$(p,\gamma)^{25}$Al	2271.3 ± 0.7	Powell et al. 1999	10	214–2312	25.0
^{25}Mg$(p,\gamma)^{26}$Al^r	6306.58 ± 0.05	Present work	81	37–1762	73.0
^{25}Mg$(p,\gamma)^{26}$Al^g	6306.58 ± 0.05	Present work	81	37–1762	...
^{25}Mg$(p,\gamma)^{26}$Al^m.....	6078.28 ± 0.05	Present work	81	37–1762	...
^{26}Mg$(p,\gamma)^{27}$Al	8271.3 ± 0.2	Present work	133	16–2867	74.5
^{23}Al$(p,\gamma)^{24}$Si	3301 ± 32	Schatz et al. 1997	4	140–1169	4.6
^{24}Al$(p,\gamma)^{25}$Si	3409 ± 11	Herndl et al. 1995	5	190–730	27.0
^{25}Al$(p,\gamma)^{26}$Si	5517.8 ± 3.1	Iliadis et al. 1996	7	44–934	27.0
^{26}Al$^g(p,\gamma)^{27}$Si	7463.1 ± 0.2	Vogelaar et al. 2001	18	5–895	80.0[b]
^{26}Al$^m(p,\gamma)^{27}$Si	7234.8 ± 0.2	Angulo et al. 1999	...	...	...
^{27}Al$(p,\gamma)^{28}$Si	11584.9 ± 0.1	Present work	105	72–3819	101.0
^{27}Al$(p,\alpha)^{24}$Mg	1600.6 ± 0.2	Present work	90	72–2967	...
^{26}Si$(p,\gamma)^{27}$P	859 ± 27	Caggiano et al. 2001	2	222–763	36.3
^{27}Si$(p,\gamma)^{28}$P	2065.5 ± 3.7	Iliadis et al. 1999	13	38–1446	78.7
^{28}Si$(p,\gamma)^{29}$P	2748.1 ± 0.7	Angulo et al. 1999	10	357–2994	44.2
^{29}Si$(p,\gamma)^{30}$P	5594.5 ± 0.4	Present work	79	107–3076	104.5
^{30}Si$(p,\gamma)^{31}$P	7297.1 ± 0.2	Present work	98	52–2929	220.0
^{27}P$(p,\gamma)^{28}$S	2463 ± 164	Herndl et al. 1995	1	1100	20.0
^{28}P$(p,\gamma)^{29}$S	3287 ± 50	Statistical model	...	...	...
^{29}P$(p,\gamma)^{30}$S	4399.9 ± 3.1	Present work	6	333–1833	73.0
^{30}P$(p,\gamma)^{31}$S	6133.3 ± 1.5	Statistical model	...	...	...
^{31}P$(p,\gamma)^{32}$S	8863.9 ± 0.2	Present work	42	160–1963	186.0
^{31}P$(p,\alpha)^{28}$Si	1915.9 ± 0.2	Present work	25	160–1963	...
^{30}S$(p,\gamma)^{31}$Cl	291 ± 50	Present work	2	330–1109	5.1
^{31}S$(p,\gamma)^{32}$Cl	1574.7 ± 6.9	Iliadis et al. 1999	10	158–1602	75.1
^{32}S$(p,\gamma)^{33}$Cl	2276.5 ± 0.5	Present work	14	75–2470	106.0
^{33}S$(p,\gamma)^{34}$Cl	5143.30 ± 0.05	Statistical model	...	...	...
^{34}S$(p,\gamma)^{35}$Cl	6370.63 ± 0.09	Statistical model	...	...	...
^{31}Cl$(p,\gamma)^{32}$Ar	2404 ± 71	Herndl et al. 1995	1	1616	54.0
^{32}Cl$(p,\gamma)^{33}$Ar	3340 ± 31	Herndl et al. 1995	5	90–1390	44.0
^{33}Cl$(p,\gamma)^{34}$Ar	4663.7 ± 3.0	Statistical model	...	...	...
^{34}Cl$(p,\gamma)^{35}$Ar	5896.6 ± 0.8	Statistical model	...	...	...
^{35}Cl$(p,\gamma)^{36}$Ar	8505.9 ± 0.3	Present work	91	50–2828	425.0
^{35}Cl$(p,\alpha)^{32}$S	1866.5 ± 0.1	Present work	94	50–2838	...
^{34}Ar$(p,\gamma)^{35}$K	78 ± 20	Herndl et al. 1995	1	1490	11.2
^{35}Ar$(p,\gamma)^{36}$K	1665.8 ± 7.8	Iliadis et al. 1999	4	4–744	124.0
^{36}Ar$(p,\gamma)^{37}$K	1857.77 ± 0.09	Present work	10	312–2575	119.5
^{35}K$(p,\gamma)^{36}$Ca	2561 ± 45	Present work	1	700	27.2
^{36}K$(p,\gamma)^{37}$Ca	3025 ± 24	Statistical model	...	...	...
^{37}K$(p,\gamma)^{38}$Ca	4548.8 ± 4.5	Statistical model	...	...	...
^{38}K$(p,\gamma)^{39}$Ca	5763.5 ± 1.9	Statistical model	...	...	...
^{39}K$(p,\gamma)^{40}$Ca	8328.24 ± 0.09	Statistical model	...	...	...
^{39}K$(p,\alpha)^{36}$Ar	1287.6 ± 0.4	Statistical model	...	...	...
^{39}Ca$(p,\gamma)^{40}$Sc.....	539.1 ± 4.4	Iliadis et al. 1999	4	233–1128	37.5
^{40}Ca$(p,\gamma)^{41}$Sc.....	1085.07 ± 0.09	Present work	8	631–1887	19.2

[a] From Audi & Wapstra 1995, except for ^{22}Mg + p and ^{26}Si + p (see Caggiano et al. 2001).

[b] Values based on theoretical estimates. For ^{22}Na + p, a value of 0.1 has been assumed in Seuthe et al. 1990 for the dimensionless reduced proton widths; for ^{26}Al^g + p, all spectroscopic factors in Champagne, Brown, & Sherr 1993 were obtained from shell model calculations.

TABLE 3

RECOMMENDED REACTION RATES $N_A\langle\sigma v\rangle_{gs}$ IN cm^3 mol^{-1} s^{-1}

T_9 (GK)	^{20}Ne(p,γ)	^{21}Ne(p,γ)	^{22}Ne(p,γ)	^{20}Na(p,γ)	^{21}Na(p,γ)	^{22}Na(p,γ)	^{23}Na(p,γ)	^{23}Na(p,α)
0.01	...	4.40E−25	8.53E−25	2.33E−25	5.99E−33	...	1.66E−32	5.67E−30
0.015.....	3.52E−24	1.47E−22	4.11E−19	6.42E−21	8.52E−28	6.48E−22	2.42E−27	1.18E−24
0.02	3.01E−21	2.91E−21	2.51E−16	9.37E−19	1.50E−24	1.36E−18	4.29E−24	1.18E−21
0.03	1.37E−17	9.41E−18	1.29E−13	1.15E−16	1.74E−20	6.15E−15	5.07E−20	1.02E−17
0.04	2.72E−15	4.49E−13	2.56E−12	1.75E−15	6.29E−18	1.06E−12	1.16E−16	3.81E−15
0.05	1.15E−13	3.57E−10	1.43E−11	9.14E−13	4.26E−16	2.57E−11	1.78E−13	2.78E−13
0.06	2.00E−12	2.92E−08	4.49E−11	1.10E−10	4.88E−14	2.09E−10	2.50E−11	8.71E−12
0.07	1.94E−11	6.56E−07	1.13E−10	3.25E−09	1.10E−11	9.36E−10	8.31E−10	3.65E−10
0.08	1.26E−10	6.58E−06	3.39E−10	4.02E−08	7.29E−10	4.40E−09	1.12E−08	7.77E−09
0.09	6.15E−10	3.87E−05	1.40E−09	2.79E−07	1.87E−08	4.57E−08	8.28E−08	8.85E−08
0.1	2.40E−09	1.57E−04	6.34E−09	1.29E−06	2.47E−07	4.86E−07	4.06E−07	6.27E−07
0.15	2.88E−07	9.68E−03	1.52E−06	1.11E−04	4.98E−04	7.33E−04	8.70E−05	2.89E−04
0.2	5.91E−06	1.08E−01	3.68E−05	9.11E−04	1.99E−02	2.76E−02	7.92E−03	1.47E−02
0.3	3.32E−04	4.17E+00	1.65E−02	6.30E−03	7.26E−01	1.07E+00	1.17E+00	1.55E+00
0.4	4.60E−03	3.18E+01	7.74E−01	1.96E−02	4.58E+00	6.86E+00	1.31E+01	1.81E+01
0.5	2.60E−02	1.05E+02	7.97E+00	1.04E−01	*1.70E+01*	2.13E+01	5.25E+01	1.00E+02
0.6	8.73E−02	2.37E+02	3.84E+01	5.42E−01	*4.44E+01*	4.66E+01	1.28E+02	4.10E+02
0.7	2.18E−01	4.34E+02	1.21E+02	1.91E+00	*9.08E+01*	8.42E+01	2.39E+02	1.27E+03
0.8	4.66E−01	7.06E+02	2.91E+02	*3.11E+00*	*1.58E+02*	1.35E+02	3.82E+02	3.15E+03
0.9	9.28E−01	1.06E+03	5.87E+02	*4.57E+00*	*2.45E+02*	2.01E+02	5.53E+02	6.55E+03
1.0	1.79E+00	1.52E+03	1.04E+03	*6.26E+00*	*3.51E+02*	2.81E+02	7.52E+02	1.20E+04
1.5	2.75E+01	5.12E+03	6.51E+03	*1.63E+01*	*1.07E+03*	*1.12E+03*	2.19E+03	9.30E+04
2.0	1.40E+02	1.00E+04	1.73E+04	*2.66E+01*	*1.88E+03*	*2.43E+03*	4.40E+03	3.20E+05
3.0	7.49E+02	*1.58E+04*	*3.67E+04*	*4.37E+01*	*3.31E+03*	*5.72E+03*	1.04E+04	*1.55E+06*
4.0	1.77E+03	*1.95E+04*	*5.77E+04*	*5.67E+01*	*4.36E+03*	*9.31E+03*	*1.49E+04*	*4.17E+06*
5.0	2.98E+03	*2.25E+04*	*8.03E+04*	*6.74E+01*	*5.16E+03*	*1.29E+04*	*1.90E+04*	*8.63E+06*
6.0	4.26E+03	*2.54E+04*	*1.03E+05*	*7.64E+01*	*5.80E+03*	*1.65E+04*	*2.30E+04*	*1.53E+07*
7.0	5.52E+03	*2.82E+04*	*1.25E+05*	*8.47E+01*	*6.35E+03*	*2.00E+04*	*2.65E+04*	*2.42E+07*
8.0	6.75E+03	*3.00E+04*	*1.40E+05*	*9.22E+01*	*6.86E+03*	*2.34E+04*	*2.92E+04*	*3.44E+07*
9.0	7.95E+03	*3.09E+04*	*1.44E+05*	*9.93E+01*	*7.34E+03*	*2.68E+04*	*3.10E+04*	*4.40E+07*
10.0	9.14E+03	*3.13E+04*	*1.49E+05*	*1.06E+02*	*7.82E+03*	*3.02E+04*	*3.13E+04*	*5.07E+07*

NOTE.—Table 3 is also available in machine-readable form in the electronic edition of the *Astrophysical Journal*.

the Maxwell-Boltzmann distribution and the partial widths are negligible over the width of the resonance. The value of the Maxwell-Boltzmann distribution at the resonance energy appears in equation (9) and, consequently, the above expression takes only the reaction rate contribution at the resonance energy into account.

2.2. *Broad-Resonance Rates*

The narrow-resonance reaction rate formalism neglects the energy dependence of the Maxwell-Boltzmann distribution. If the bombarding energy is continuously decreased below the resonance energy E_R, then the product of resonant cross section and Maxwell-Boltzmann distribution may produce another peak at energies different from E_R. According to equation (1), there will be another contribution to the total resonant reaction rate arising from the wing of the resonance, which is neglected in equation (9). According to Burbidge et al. (1967), if a resonance E_R falls within the range $E_0 \pm 2\Delta$ of the Gamow peak, then the narrow-resonance reaction rate formalism given by equation (9) will represent a reliable approximation to the total resonance reaction rates. Otherwise, the wing of the resonance has to be taken into account.

The cross section for a broad (p,γ) or (p,α) resonance is calculated by using the Breit-Wigner formula

$$\sigma(E) = \frac{\lambda^2}{4\pi}\,\frac{2J_R+1}{(2j_t+1)(2j_p+1)}\,\frac{\Gamma_p(E)\Gamma_x(E)}{(E_R-E)^2+\frac{1}{4}\Gamma(E)^2}\,, \qquad (10)$$

where J_R, j_t, and j_p are the spin of the resonance, target, and proton, respectively, λ is the de Broglie wavelength of the protons, Γ_p is the proton partial width, Γ_x is the γ-ray or α-particle partial width, and Γ is the total resonance width (Blatt & Weisskopf 1952). The partial widths describe the probability of decay or formation of the resonance through a particle or γ-ray channel. The energy dependences of the proton (or α-particle) and γ-ray partial widths are given by

$$\Gamma_p(E) = \Gamma_p(E_R)\,\frac{P(E)}{P(E_R)}\,, \qquad (11)$$

$$\Gamma_\gamma(E) = \Gamma_\gamma(E_R)B_\gamma\left(\frac{E+Q_{p\gamma}-E_{xf}}{E_R+Q_{p\gamma}-E_{xf}}\right)^{2L+1}\,, \qquad (12)$$

where $Q_{p\gamma}$ is the reaction Q-value, B_γ is the primary γ-ray branching ratio to the final state at E_{xf}, and L is the multipolarity of the γ-ray transition. The penetration factors, P, are calculated with channel radius parameters of $a_0 = 1.25$ or 1.40 fm for protons and α-particles, respectively. Note that all widths in equations (10)–(12) are "observed" R matrix quantities (Lane & Thomas 1958).

With the resonant cross section given by equation (10), the reaction rates for a transition to a specific final state have been calculated either by parameterizing the S-factor wing according to equation (3) and using the nonresonant reaction rate formalism or by integrating equation (1) numerically. The total reaction rates were obtained by

TABLE 4

RECOMMENDED REACTION RATES $N_A\langle\sigma v\rangle_{gs}$ IN cm^3 mol^{-1} s^{-1}

T_9 (GK)	^{22}Mg(p,γ)	^{23}Mg(p,γ)	^{24}Mg(p,γ)	^{25}Mg$(p,\gamma)^{t*}$	^{25}Mg$(p,\gamma)^{g*}$	^{25}Mg$(p,\gamma)^{m*}$	^{26}Mg(p,γ)	^{23}Al(p,γ)
0.01	1.57E−36	4.95E−35	...	6.74E−34	5.39E−34	1.35E−34	1.50E−34	3.98E−38
0.015.....	4.69E−31	1.47E−29	...	1.29E−24	1.05E−24	2.42E−25	3.96E−27	2.41E−32
0.02	1.32E−27	4.15E−26	5.27E−26	5.57E−20	4.53E−20	1.04E−20	6.77E−23	1.06E−28
0.03	2.76E−23	8.67E−22	1.14E−21	1.99E−15	1.64E−15	3.50E−16	1.53E−18	5.96E−22
0.04	1.45E−20	4.54E−19	6.26E−19	3.43E−13	2.79E−13	6.41E−14	2.29E−15	2.92E−16
0.05	1.25E−18	3.88E−17	1.06E−16	7.66E−12	6.26E−12	1.40E−12	3.12E−13	7.03E−13
0.06	3.70E−17	1.14E−15	1.51E−13	7.18E−11	5.92E−11	1.26E−11	8.69E−12	1.20E−10
0.07	5.52E−16	1.70E−14	4.41E−11	4.32E−10	3.59E−10	7.27E−11	1.04E−10	4.57E−09
0.08	5.13E−15	1.58E−13	3.05E−09	1.87E−09	1.56E−09	3.07E−10	7.92E−10	6.81E−08
0.09	3.37E−14	1.03E−12	8.04E−08	6.34E−09	5.23E−09	1.11E−09	4.66E−09	5.45E−07
0.1	1.70E−13	5.19E−12	1.09E−06	1.74E−08	1.44E−08	2.96E−09	2.28E−08	2.83E−06
0.15	5.13E−11	1.53E−09	2.33E−03	6.52E−06	5.46E−06	1.06E−06	2.40E−05	3.46E−04
0.2	1.89E−09	9.45E−08	9.52E−02	1.28E−03	1.10E−03	1.82E−04	4.38E−03	3.37E−03
0.3	2.08E−07	2.33E−04	3.25E+00	2.81E−01	2.38E−01	4.33E−02	1.08E+00	2.75E−02
0.4	4.42E−06	1.52E−02	1.70E+01	4.23E+00	3.51E+00	7.18E−01	1.66E+01	6.93E−02
0.5	3.43E−05	1.78E−01	4.32E+01	2.23E+01	1.82E+01	4.11E+00	8.38E+01	1.12E−01
0.6	1.49E−04	8.93E−01	7.85E+01	6.92E+01	5.54E+01	1.38E+01	2.43E+02	1.46E−01
0.7	4.58E−04	2.76E+00	1.19E+02	1.60E+02	1.26E+02	3.42E+01	5.16E+02	1.71E−01
0.8	1.14E−03	6.39E+00	1.61E+02	3.02E+02	2.33E+02	6.86E+01	8.99E+02	1.90E−01
0.9	2.48E−03	1.21E+01	2.05E+02	5.03E+02	3.83E+02	1.20E+02	1.38E+03	2.06E−01
1.0	4.87E−03	*1.71E+01*	2.51E+02	7.61E+02	5.72E+02	1.89E+02	1.94E+03	2.22E−01
1.5	5.74E−02	*5.19E+01*	5.14E+02	2.80E+03	2.00E+03	7.98E+02	5.39E+03	*1.01E+00*
2.0	3.08E−01	*9.61E+01*	8.50E+02	5.68E+03	3.94E+03	1.74E+03	9.46E+03	*2.28E+00*
3.0	2.54E+00	*1.88E+02*	*2.04E+03*	*1.03E+04*	*7.16E+03*	*3.14E+03*	1.97E+04	*5.35E+00*
4.0	8.84E+00	*2.77E+02*	*3.37E+03*	*1.45E+04*	*1.00E+04*	*4.50E+03*	*3.55E+04*	*8.31E+00*
5.0	2.04E+01	*3.63E+02*	*4.73E+03*	*1.91E+04*	*1.32E+04*	*5.90E+03*	*5.27E+04*	*1.09E+01*
6.0	3.75E+01	*4.48E+02*	*5.99E+03*	*2.35E+04*	*1.63E+04*	*7.20E+03*	*7.00E+04*	*1.31E+01*
7.0	6.05E+01	*5.38E+02*	*7.18E+03*	*2.78E+04*	*1.93E+04*	*8.50E+03*	*8.64E+04*	*1.52E+01*
8.0	8.97E+01	*6.30E+02*	*8.31E+03*	*3.12E+04*	*2.16E+04*	*9.60E+03*	*1.01E+05*	*1.69E+01*
9.0	1.25E+02	*7.27E+02*	*9.39E+03*	*3.27E+04*	*2.26E+04*	*1.01E+04*	*1.15E+05*	*1.85E+01*
10.0	1.67E+02	*8.28E+02*	*1.04E+04*	*3.31E+04*	*2.30E+04*	*1.04E+04*	*1.27E+05*	*1.99E+01*

NOTE.—Table 4 is also available in machine-readable form in the electronic edition of the *Astrophysical Journal*.

summing the contributions of transitions to different final states.

2.3. *Direct Proton Capture*

Reaction rates for direct proton capture can be calculated by using the nonresonant reaction rate formalism, since the cross section (or S-factor) varies smoothly with energy. The cross section for direct proton capture has been estimated by using a single-particle potential model. The dominant $E1$ contribution to the (p,γ) cross section (in microbarns) for capture from an initial scattering state to a final bound state with orbital angular momenta of l_i and l_f, respectively, is given by

$$\sigma(E1, l_i l_f) = 0.0716\mu^{3/2}\left(\frac{Z_p}{M_p} - \frac{Z_t}{M_t}\right)^2 \times \frac{E_\gamma^3}{E^{3/2}} \frac{(2J_f+1)(2l_i+1)}{(2j_p+1)(2j_t+1)(2l_f+1)} \times (l_i 010 \,|\, l_f 0)^2 R_{l_i 1 l_f}^2 , \quad (13)$$

$$R_{l_i\, 1 l_f} = \int_0^\infty u_c(r) O_{E1}(r) u_b(r) r^2\, dr , \quad (14)$$

where Z_p, Z_t, M_p, and M_t are the charges and masses (in atomic mass units) of projectile and target; j_p, j_t, and J_f are the spins of projectile, target, and final state, respectively; O_{E1} is the radial part of the $E1$ multipole operator; and u_c and u_b the radial wave functions of the initial scattering state and final bound state, respectively.

In the present work, the scattering-state wave functions have been calculated by using phase shifts for a hard sphere in a Coulomb potential. Furthermore, the bound-state wave functions were generated by using a Woods-Saxon potential with radius parameter $r_0 = 1.25$ fm and diffuseness $a = 0.65$ fm. The well depths were chosen to reproduce the binding energies of the final states. In the past, several researchers have employed bound-state square-well potentials instead of Woods-Saxon potentials (see, for example, Rolfs 1973; Trautvetter & Rolfs 1975). However, it was shown recently (Wiescher et al. 1980; Powell et al. 1999) that the use of square-well potentials sometimes overpredicts calculated single-particle direct capture cross sections by a factor of 3.

The total direct capture cross section is given by an incoherent sum over all orbital angular momenta l_i and l_f and over all final bound states j

$$\sigma_{\rm total}^{\rm DC} = \sum_j \sum_{l_i l_f} C^2 S_j(l_f) \sigma_{{\rm calc},\, j}^{\rm DC}(l_i, l_f) , \quad (15)$$

where $S(l_f)$ and C denote the single-particle spectroscopic factor and the isospin Clebsch-Gordan coefficient, respectively.

TABLE 5

RECOMMENDED REACTION RATES $N_A\langle\sigma v\rangle_{gs}$ IN cm^3 mol^{-1} s^{-1}

T_9 (GK)	^{24}Al (p,γ)	^{25}Al(p,γ)	^{26}Al$^g(p,\gamma)$	^{26}Al$^m(p,\gamma)$	^{27}Al(p,γ)*	^{27}Al(p,α)*	^{26}Si(p,γ)	^{27}Si(p,γ)
0.01	2.18E−37	5.53E−36	5.78E−37	...	6.87E−37	2.65E−40	4.70E−40	9.15E−33
0.015.....	1.33E−31	7.17E−29	1.42E−29	...	4.74E−31	1.87E−31	6.71E−34	1.41E−26
0.02	5.92E−28	2.31E−25	5.50E−24	*9.17E−24*	3.50E−26	1.29E−25	5.09E−30	1.54E−23
0.03	2.19E−23	6.45E−22	1.86E−18	*2.61E−18*	2.62E−20	7.85E−20	3.69E−25	5.35E−20
0.04	1.65E−20	4.45E−20	1.09E−15	*1.40E−15*	3.01E−17	6.08E−17	4.26E−22	4.61E−17
0.05	2.03E−18	2.03E−18	6.38E−14	*7.78E−14*	2.29E−15	3.39E−15	6.39E−20	3.22E−15
0.06	2.98E−16	6.52E−17	1.35E−12	*1.59E−12*	4.82E−14	5.03E−14	2.91E−18	1.22E−13
0.07	3.62E−14	1.12E−15	2.64E−11	*3.11E−11*	1.60E−12	3.48E−13	6.11E−17	4.23E−12
0.08	1.48E−12	1.19E−14	6.27E−10	*7.52E−10*	6.73E−11	1.59E−12	7.69E−16	7.39E−11
0.09	2.64E−11	8.72E−14	9.84E−09	*1.19E−08*	1.41E−09	7.03E−12	9.61E−15	6.91E−10
0.1	2.61E−10	4.84E−13	9.30E−08	*1.12E−07*	1.65E−08	3.79E−11	2.67E−13	4.09E−09
0.15	2.22E−07	3.94E−10	7.76E−05	*9.86E−05*	2.51E−05	2.76E−08	6.38E−08	7.72E−07
0.2	6.29E−06	6.31E−07	2.52E−03	*3.55E−03*	9.62E−04	8.88E−07	2.98E−05	2.05E−05
0.3	1.11E−03	1.83E−03	1.56E−01	*2.79E−01*	4.25E−02	6.94E−04	1.16E−02	4.76E−03
0.4	3.78E−02	8.93E−02	1.88E+00	*4.14E+00*	3.96E−01	5.15E−02	2.02E−01	8.48E−02
0.5	3.22E−01	8.58E−01	9.07E+00	...	2.08E+00	6.81E−01	1.04E+00	4.60E−01
0.6	*9.79E−01*	3.69E+00	2.59E+01	...	7.70E+00	3.86E+00	2.95E+00	1.39E+00
0.7	*2.25E+00*	1.01E+01	5.41E+01	...	2.18E+01	1.37E+01	5.99E+00	3.07E+00
0.8	*4.31E+00*	*1.97E+01*	*1.11E+02*	...	5.06E+01	3.68E+01	9.93E+00	5.55E+00
0.9	*7.22E+00*	*3.37E+01*	*2.00E+02*	...	1.00E+02	8.39E+01	1.44E+01	8.84E+00
1.0	*1.11E+01*	*5.21E+01*	*3.21E+02*	...	1.79E+02	1.72E+02	1.90E+01	1.28E+01
1.5	*4.22E+01*	*2.04E+02*	*1.47E+03*	...	1.12E+03	2.71E+03	3.91E+01	*4.91E+01*
2.0	*8.55E+01*	*4.19E+02*	*3.31E+03*	...	3.04E+03	1.69E+04	5.07E+01	*1.00E+02*
3.0	*1.80E+02*	*8.84E+02*	*7.75E+03*	...	8.90E+03	1.45E+05	6.69E+01	*2.21E+02*
4.0	*2.65E+02*	*1.31E+03*	*1.20E+04*	...	1.54E+04	*5.04E+05*	1.04E+02	*3.49E+02*
5.0	*3.39E+02*	*1.67E+03*	*1.57E+04*	...	*2.07E+04*	*1.35E+06*	1.86E+02	*4.80E+02*
6.0	*4.07E+02*	*1.99E+03*	*1.90E+04*	...	*2.63E+04*	*2.93E+06*	3.31E+02	*6.15E+02*
7.0	*4.66E+02*	*2.28E+03*	*2.18E+04*	...	*3.11E+04*	*5.50E+06*	5.49E+02	*7.55E+02*
8.0	*5.22E+02*	*2.53E+03*	*2.44E+04*	...	*3.50E+04*	*8.82E+06*	8.47E+02	*8.99E+02*
9.0	*5.75E+02*	*2.77E+03*	*2.67E+04*	...	*3.66E+04*	*1.21E+07*	1.23E+03	*1.04E+03*
10.0	*6.25E+02*	*2.99E+03*	*2.89E+04*	...	*3.71E+04*	*1.41E+07*	1.69E+03	*1.19E+03*

NOTE.—Table 5 is also available in machine-readable form in the electronic edition of the *Astrophysical Journal*.

3. PROCEDURES

3.1. *General Remarks*

For each reaction under consideration, the available experimental nuclear structure and reaction information (for example, resonance energies, strengths, partial widths, and spectroscopic factors) is different. Consequently there is no unique prescription for calculating reaction rates. However, the methods applied here can be roughly divided into two classes, depending on the stability of the target nuclei involved in the reaction. In this section we summarize our procedures for both cases.

For stable targets (including the long-lived ^{22}Na and ^{26}Al nuclei), we first collected the available information on measured resonance energies and strengths. The latter values were normalized to a standard set of absolute resonance strengths. The experimental resonance strength standards adopted here are discussed in more detail in § 3.2. Subsequently, we collected all available information on compound nuclear states located between the proton threshold and the lowest-lying observed resonance. The resonance energies have been calculated from the measured excitation energies and the reaction Q-values, i.e., $E_R = E_x - Q$. The corresponding resonance strengths were estimated by using proton spectroscopic factors measured in transfer reaction studies. This procedure is discussed in more detail in § 3.3. With this information, the narrow resonance reaction rates have been calculated according to equation (9). Cross sections for low-energy wings of broad resonances and high-energy wings of subthresold resonances were estimated by using experimental information on resonance parameters. The resulting reaction rate contributions were estimated by using the formalism presented in § 2.2. In addition, for (p,γ) reactions the direct capture reaction rates have been either extrapolated to lower energies using equation (13) (for example, the experimental DC cross sections have been measured for ^{24}Mg + p, ^{28}Si + p, and ^{32}S + p) or were calculated[1] from measured nuclear structure information according to equation (15). On the basis of available data, upper and lower limits of total reaction rates have been calculated (§ 3.5). In agreement with the method described in Angulo et al. (1999), recommended reaction rates were estimated by multiplying the parameters (e.g., resonance strengths) that give rise to the upper limits by a factor of 0.1.

For short-lived target nuclei in the A = 20–40 range, no experimental information on resonance energies, strengths, or cross sections is available. The compound nuclei of interest here are proton-rich and have been investigated only through a restricted number of reactions involving stable beams and targets. For this reason, the nuclear structure above the proton threshold is poorly known and in many cases only information on excitation energies and spin-parity restrictions for a few unbound levels is available. Fortunately, the astrophysically interesting compound nuclei have mirror counterparts that are experimentally

[1] We estimated an error of 30% for the calculated direct capture reaction rates.

TABLE 6

RECOMMENDED REACTION RATES $N_A\langle\sigma v\rangle_{gs}$ IN cm^3 mol^{-1} s^{-1}

T_9 (GK)	^{28}Si(p,γ)	^{29}Si(p,γ)*	^{30}Si(p,γ)*	^{27}P(p,γ)	^{28}P(p,γ)	^{29}P(p,γ)*	^{30}P(p,γ)	^{31}P(p,γ)*
0.01	...	2.86E−39	1.23E−35	3.00E−42	...	9.87E−42	...	2.31E−41
0.015.....	...	3.59E−33	3.53E−27	7.32E−36	...	2.43E−35	...	5.75E−35
0.02	...	2.53E−29	5.25E−23	7.79E−32	...	2.60E−31	...	6.20E−31
0.03	5.97E−25	1.17E−22	6.54E−19	8.64E−27	...	2.91E−26	...	6.99E−26
0.04	6.61E−22	2.39E−18	6.42E−17	1.31E−23	...	4.41E−23	...	1.11E−22
0.05	9.63E−20	8.61E−16	9.33E−16	2.37E−21	...	8.01E−21	...	1.90E−19
0.06	4.29E−18	4.14E−14	5.31E−15	1.25E−19	...	4.22E−19	...	2.24E−16
0.07	8.87E−17	6.36E−13	1.82E−14	2.95E−18	...	9.98E−18	...	3.80E−14
0.08	1.08E−15	4.81E−12	4.98E−14	4.00E−17	...	1.36E−16	...	1.76E−12
0.09	9.01E−15	2.31E−11	1.53E−13	3.62E−16	...	1.42E−15	...	3.41E−11
0.1	6.44E−14	9.03E−11	6.04E−13	2.41E−15	...	2.07E−14	...	3.61E−10
0.15	5.46E−09	1.07E−06	8.58E−10	1.92E−12	...	2.70E−09	...	4.04E−07
0.2	3.59E−06	3.21E−04	1.41E−06	1.28E−10	...	1.10E−06	...	2.75E−05
0.3	1.98E−03	1.05E−01	3.22E−03	2.44E−08	...	4.03E−04	*4.20E−03*	9.10E−03
0.4	4.11E−02	2.11E+00	1.73E−01	6.59E−07	...	8.12E−03	*1.00E−01*	2.16E−01
0.5	2.35E−01	1.29E+01	2.14E+00	6.81E−06	...	5.47E−02	*8.52E−01*	1.55E+00
0.6	7.14E−01	4.23E+01	1.22E+01	4.02E−05	...	2.08E−01	*3.98E+00*	6.04E+00
0.7	1.52E+00	9.75E+01	4.31E+01	1.65E−04	...	5.58E−01	*1.27E+01*	1.62E+01
0.8	2.62E+00	1.79E+02	1.11E+02	5.30E−04	...	1.18E+00	*3.17E+01*	3.43E+01
0.9	3.92E+00	2.85E+02	2.34E+02	1.42E−03	...	2.14E+00	*6.60E+01*	6.19E+01
1.0	5.33E+00	4.10E+02	4.22E+02	3.31E−03	...	3.47E+00	*1.21E+02*	9.96E+01
1.5	1.29E+01	1.15E+03	2.37E+03	6.44E−02	*1.18E+02*	1.53E+01	*8.21E+02*	4.39E+02
2.0	2.93E+01	1.87E+03	5.51E+03	4.07E−01	*2.60E+02*	*3.65E+01*	*2.30E+03*	*1.09E+03*
3.0	1.85E+02	3.28E+03	1.29E+04	3.99E+00	*5.88E+02*	*9.32E+01*	*6.89E+03*	*2.73E+03*
4.0	*3.82E+02*	*5.11E+03*	*2.54E+04*	1.65E+01	*9.05E+02*	*1.55E+02*	*1.24E+04*	*4.73E+03*
5.0	*6.51E+02*	*7.07E+03*	*4.04E+04*	4.47E+01	*1.20E+03*	*2.17E+02*	*1.79E+04*	*7.11E+03*
6.0	*9.92E+02*	*9.34E+03*	*5.68E+04*	9.50E+01	*1.47E+03*	*2.77E+02*	*2.31E+04*	*9.76E+03*
7.0	*1.41E+03*	*1.16E+04*	*7.39E+04*	1.72E+02	*1.73E+03*	*3.34E+02*	*2.79E+04*	*1.25E+04*
8.0	*1.90E+03*	*1.35E+04*	*9.06E+04*	2.80E+02	*1.97E+03*	*3.87E+02*	*3.23E+04*	*1.49E+04*
9.0	*2.48E+03*	*1.40E+04*	*1.07E+05*	4.19E+02	*2.21E+03*	*4.38E+02*	*3.63E+04*	*1.58E+04*
10.0	*3.16E+03*	*1.43E+04*	*1.23E+05*	5.91E+02	*2.43E+03*	*4.85E+02*	*4.00E+04*	*1.61E+04*

NOTE.—Table 6 is also available in machine-readable form in the electronic edition of the *Astrophysical Journal*.

well understood. Therefore, we collected available information on excitation energies for the mirror nuclei. Mirror state correspondences were established by using experimentally determined level energies and spin-parity restrictions. In a second step, the excitation energies of missing levels in the proton-rich nucleus have been estimated from the experimental energies of the neutron-rich mirror states by using calculated Coulomb displacement energies or by applying the isobaric multiplet mass equation (see the discussion in Iliadis et al. 1999). In a final step, the resonance parameters and cross sections for the reaction of interest were calculated from measured or estimated excitation energies in the proton-rich compound nucleus and from measured spectroscopic factors and mean lifetimes adopted from the neutron-rich mirror levels (see § 3.3). With this information given, recommended reaction rates have been calculated by applying the formalism presented in § 2.

3.2. *Absolute Resonance Strength Standards*

The strength of a resonance in a (p,γ) reaction is defined by

$$\omega\gamma = \frac{2J_R + 1}{(2j_t + 1)(2j_p + 1)} \frac{\Gamma_p \Gamma_\gamma}{\Gamma} , \qquad (16)$$

where the partial and total widths are given at the resonance energy, E_R (Gove 1959). Measurements of absolute resonance strengths are difficult, and discrepancies by factors of 2 or more between different measurements are common in the literature. Most resonance strengths are derived from the step height of thick-target yield curves (Gove 1959). This method requires knowledge of the target stoichiometry, absolute stopping powers, absolute proton charge deposited on the target, and absolute detection efficiencies. All these factors are difficult to determine and, therefore, are sources of both random and systematic errors. Relative measurements of resonance strengths are less difficult and literature values derived by different authors are usually in good agreement.

A few studies have attempted careful measurements of absolute resonance strengths by minimizing or eliminating the influence of the experimental artifacts mentioned above (Paine & Sargood 1979; Sargood 1982) A promising technique has been reported recently in Powell et al. (1998). In this study the resonant γ-rays were measured simultaneously with the number of Rutherford scattered protons, leading to the expression

$$\omega\gamma = \frac{2}{\lambda^2} \frac{1}{B_\gamma W_\gamma(\theta)} \frac{\Omega_{cm}}{\eta_\gamma} \int \frac{N_\gamma(E)}{N_{p'}(E)} \sigma_{Ruth}(E) dE , \qquad (17)$$

where N_γ, B_γ, η_γ, and W_γ are the number of observed γ-rays, the branching ratio, the detection efficiency, and the angular distribution, respectively, of the γ-ray transition under consideration and $N_{p'}$ and Ω_{cm} are the number of observed elastically scattered protons and the center-of-mass solid

TABLE 7

RECOMMENDED REACTION RATES $N_A\langle\sigma v\rangle_{gs}$ IN cm^3 mol^{-1} s^{-1}

T_9 (GK)	^{31}P(p,α)*	^{30}S(p,γ)*	^{31}S(p,γ)	^{32}S(p,γ)*	^{33}S(p,γ)	^{34}S(p,γ)	^{31}Cl(p,γ)	^{32}Cl(p,γ)
0.01	7.79E−44	3.72E−45	5.11E−44	7.00E−44	...	...	2.31E−46	1.80E−46
0.015.....	2.13E−37	1.78E−38	2.45E−37	4.43E−35	...	...	2.12E−39	2.10E−39
0.02	2.61E−33	2.91E−34	4.00E−33	6.04E−29	*4.49E−49*	...	5.22E−35	1.04E−32
0.03	3.86E−28	5.52E−29	7.61E−28	6.95E−23	*1.61E−32*	*1.06E−31*	1.66E−29	2.05E−25
0.04	2.19E−24	1.17E−25	1.21E−23	6.56E−20	*1.19E−24*	*5.27E−24*	4.89E−26	8.02E−22
0.05	1.13E−20	2.71E−23	7.34E−20	3.71E−18	*4.69E−20*	*1.45E−19*	1.43E−23	1.06E−19
0.06	4.58E−18	1.71E−21	2.54E−17	5.19E−17	*4.99E−17*	*1.17E−16*	1.08E−21	2.63E−18
0.07	3.71E−16	5.40E−20	1.60E−15	3.30E−16	*7.21E−15*	*1.38E−14*	3.41E−20	2.70E−17
0.08	1.11E−14	6.05E−18	3.48E−14	1.30E−15	*3.07E−13*	*5.06E−13*	5.87E−19	2.81E−16
0.09	1.69E−13	9.19E−16	3.74E−13	3.77E−15	*5.89E−12*	*8.71E−12*	6.50E−18	4.79E−15
0.1	1.55E−12	5.49E−14	2.46E−12	9.18E−15	*6.49E−11*	*1.06E−10*	5.15E−17	6.42E−14
0.15	3.67E−09	1.04E−08	6.11E−10	3.06E−12	*1.29E−07*	*1.29E−07*	7.61E−14	1.70E−10
0.2	2.09E−06	4.02E−06	8.57E−09	4.80E−09	*9.13E−06*	*1.07E−05*	7.51E−12	7.78E−09
0.3	1.54E−03	1.29E−03	9.41E−07	5.03E−05	*1.27E−03*	*2.59E−03*	2.33E−09	5.31E−07
0.4	4.82E−02	2.04E−02	1.57E−04	7.31E−03	*2.36E−02*	*7.54E−02*	8.56E−08	6.91E−05
0.5	5.61E−01	9.92E−02	3.65E−03	1.39E−01	*1.71E−01*	*7.46E−01*	1.10E−06	1.92E−03
0.6	3.63E+00	2.71E−01	2.94E−02	9.47E−01	*7.20E−01*	*3.93E+00*	7.70E−06	1.74E−02
0.7	1.49E+01	5.34E−01	1.28E−01	3.60E+00	*2.15E+00*	*1.38E+01*	3.62E−05	8.36E−02
0.8	4.41E+01	8.67E−01	3.83E−01	9.55E+00	*5.09E+00*	*3.72E+01*	1.29E−04	2.71E−01
0.9	1.05E+02	*1.59E+00*	8.88E−01	2.00E+01	*1.02E+01*	*8.27E+01*	3.79E−04	6.77E−01
1.0	2.17E+02	*2.65E+00*	1.73E+00	3.55E+01	*1.79E+01*	*1.60E+02*	9.55E−04	1.41E+00
1.5	3.28E+03	*1.46E+01*	1.25E+01	1.74E+02	*1.01E+02*	*1.34E+03*	2.47E−02	*9.82E+00*
2.0	*1.71E+04*	*4.00E+01*	*3.14E+01*	3.39E+02	*2.38E+02*	*4.37E+03*	1.91E−01	*2.75E+01*
3.0	*1.31E+05*	*1.36E+02*	*8.69E+01*	*1.04E+03*	*5.66E+02*	*1.65E+04*	2.38E+00	*8.16E+01*
4.0	*4.79E+05*	*2.96E+02*	*1.57E+02*	*2.01E+03*	*9.38E+02*	*3.57E+04*	1.14E+01	*1.47E+02*
5.0	*1.29E+06*	*5.25E+02*	*2.37E+02*	*3.17E+03*	*1.42E+03*	*6.02E+04*	3.42E+01	*2.17E+02*
6.0	*2.82E+06*	*8.20E+02*	*3.25E+02*	*4.49E+03*	*1.98E+03*	*8.83E+04*	7.86E+01	*2.89E+02*
7.0	*5.23E+06*	*1.18E+03*	*4.17E+02*	*5.91E+03*	*2.63E+03*	*1.19E+05*	1.52E+02	*3.60E+02*
8.0	*8.23E+06*	*1.59E+03*	*5.12E+02*	*7.40E+03*	*3.16E+03*	*1.49E+05*	2.62E+02	*4.31E+02*
9.0	*1.12E+07*	*2.05E+03*	*6.13E+02*	*8.93E+03*	*3.50E+03*	*1.80E+05*	4.14E+02	*5.00E+02*
10.0	*1.27E+07*	*2.53E+03*	*7.11E+02*	*1.05E+04*	*3.65E+03*	*2.10E+05*	6.12E+02	*5.66E+02*

NOTE.—Table 7 is also available in machine-readable form in the electronic edition of the *Astrophysical Journal*.

angle of the particle detector in steradians, respectively. It should be emphasized that the resonance strength in equation (17) is independent of the properties of the target (stoichiometry, stopping power, uniformity, and stability) and the beam (current integration and straggling). Furthermore, the value of $\omega\gamma$ depends on the ratio Ω_{cm}/η_γ and, consequently, does not require measurement of *absolute* γ-ray and charged-particle detection efficiencies. The latter ratio was measured directly in Powell et al. (1998) by using the ^{19}F$(p,\alpha_2\gamma)^{16}$O reaction. Clearly, absolute resonance strengths measured with techniques similar to the one described above are more reliable than most other studies that determine $\omega\gamma$ from the step height of thick-target yield curves.

In Table 1 we list absolute (p,γ) resonance strengths involving stable targets in the sd shell. Most values have been adopted from Paine & Sargood (1979) and from Powell et al. (1998). It should be noted that both sets of absolute resonance strengths are consistent with each other (see the discussion in Powell et al. 1998). We have also included the ^{36}Ar$(p,\gamma)^{37}$K reaction, since two groups (Goosman & Kavanagh 1967; Mohr et al. 1999) have independently measured the same resonance using different techniques (gas target and implanted target, respectively) and found consistent results. For the reactions listed in Table 1 we have normalized all available measured strengths to the corresponding standard values. Clearly, it would be desirable to extend the set of absolute strength standards to reactions not listed in Table 1, for example, to proton captures on the Ne isotopes. Note that our approach differs from the procedure in Angulo et al. (1999) in which all available sets of resonance strength measurements have simply been averaged.

3.3. *Proton Partial Widths and Spectroscopic Factors*

Spectroscopic factors represent important information for the calculation of reaction rates for two major reasons. First, their values are frequently needed in order to compute the direct capture contribution to the reaction rates according to equation (15). Second, they can be used to estimate proton partial widths. The latter quantity, in turn, is needed for calculating resonant reaction rates according to equations (9) and (16). Furthermore, at low resonance energies the proton partial width alone determines the resonance strength, since the relation $\Gamma_p \ll \Gamma_\gamma$ reduces equation (9) to $\omega\gamma \approx \omega\Gamma_p$.

A reliable method for calculating a proton partial width for a given spectroscopic factor is described by

$$\Gamma_p = C^2 S \Gamma_{sp} , \tag{18}$$

where Γ_{sp} denotes the partial width of a single-particle resonance located at the same energy as the resonance of interest (Schiffer 1963). The value of Γ_{sp} can be computed numerically by solving the Schrödinger equation for the elastic scattering of protons by an appropriate diffuse-edge optical model potential. Alternatively, the proton partial

TABLE 8

RECOMMENDED REACTION RATES $N_A\langle\sigma v\rangle_{gs}$ IN $cm^3\ mol^{-1}\ s^{-1}$

T_9 (GK)	$^{33}Cl(p,\gamma)$	$^{34}Cl(p,\gamma)$	$^{35}Cl(p,\gamma)$*	$^{35}Cl(p,\alpha)$*	$^{34}Ar(p,\gamma)$	$^{35}Ar(p,\gamma)$	$^{36}Ar(p,\gamma)$*	$^{35}K(p,\gamma)$*
0.01	...	...	9.67E−41	6.74E−43	2.87E−49	2.98E−48	2.81E−48	4.98E−51
0.015.....	...	...	1.13E−32	7.84E−35	5.06E−42	5.23E−41	4.97E−41	1.64E−43
0.02	...	...	1.08E−28	7.45E−31	1.88E−37	1.93E−36	1.85E−36	9.05E−39
0.03	...	...	8.62E−25	5.93E−27	1.00E−31	1.02E−30	9.83E−31	7.93E−33
0.04	...	...	7.88E−23	5.95E−25	4.07E−28	4.52E−27	3.99E−27	4.42E−29
0.05	...	...	1.18E−19	1.42E−21	1.50E−25	1.31E−22	1.46E−24	2.03E−26
0.06	...	...	5.49E−17	6.64E−19	1.35E−23	5.76E−19	1.75E−22	2.18E−24
0.07	...	...	4.29E−15	5.18E−17	4.92E−22	2.24E−16	1.99E−19	9.09E−23
0.08	...	...	1.09E−13	1.32E−15	9.52E−21	1.91E−14	1.03E−16	1.97E−21
0.09	...	...	1.33E−12	1.62E−14	1.16E−19	5.95E−13	1.33E−14	2.65E−20
0.1	...	...	9.77E−12	1.18E−13	1.00E−18	9.14E−12	6.37E−13	2.48E−19
0.15	...	...	6.79E−09	1.96E−10	2.00E−15	2.91E−08	6.15E−08	6.63E−16
0.2	...	*3.70E−06*	1.14E−06	7.72E−08	2.39E−13	1.44E−06	1.68E−05	1.10E−13
0.3	...	*1.14E−03*	9.41E−04	5.86E−05	9.43E−11	6.01E−05	3.86E−03	6.15E−09
0.4	...	*3.86E−02*	4.04E−02	3.32E−03	4.03E−09	3.49E−04	5.14E−02	3.46E−06
0.5	...	*4.24E−01*	4.09E−01	5.94E−02	5.78E−08	1.14E−03	2.26E−01	1.43E−04
0.6	...	*2.40E+00*	1.97E+00	4.68E−01	4.38E−07	*4.95E−03*	5.79E−01	1.64E−03
0.7	...	*8.91E+00*	6.26E+00	2.15E+00	2.20E−06	*1.48E−02*	1.11E+00	9.00E−03
0.8	...	*2.48E+01*	1.53E+01	6.92E+00	8.31E−06	*3.45E−02*	1.83E+00	3.14E−02
0.9	...	*5.67E+01*	3.17E+01	1.74E+01	2.55E−05	*6.84E−02*	2.81E+00	8.14E−02
1.0	...	*1.12E+02*	5.79E+01	3.70E+01	6.77E−05	*1.19E−01*	4.24E+00	1.71E−01
1.5	...	*9.51E+02*	4.07E+02	4.20E+02	2.14E−03	*6.99E−01*	2.67E+01	1.40E+00
2.0	*2.40E+02*	*2.99E+03*	1.16E+03	1.94E+03	1.83E−02	*1.84E+00*	8.45E+01	3.53E+00
3.0	*7.21E+02*	*9.83E+03*	*3.03E+03*	*1.66E+04*	2.47E−01	*5.45E+00*	*3.04E+02*	7.68E+00
4.0	*1.31E+03*	*1.80E+04*	*5.31E+03*	*7.51E+04*	1.22E+00	*1.04E+01*	*6.50E+02*	1.09E+01
5.0	*1.94E+03*	*2.58E+04*	*8.15E+03*	*2.45E+05*	3.82E+00	*1.63E+01*	*1.09E+03*	1.51E+01
6.0	*2.58E+03*	*3.28E+04*	*1.16E+04*	*6.28E+05*	9.09E+00	*2.31E+01*	*1.63E+03*	2.25E+01
7.0	*3.22E+03*	*3.89E+04*	*1.55E+04*	*1.34E+06*	1.80E+01	*3.06E+01*	*2.23E+03*	3.52E+01
8.0	*3.86E+03*	*4.42E+04*	*1.83E+04*	*2.29E+06*	3.18E+01	*3.85E+01*	*2.86E+03*	5.52E+01
9.0	*4.49E+03*	*4.89E+04*	*1.98E+04*	*3.21E+06*	5.15E+01	*4.66E+01*	*3.53E+03*	8.44E+01
10.0	*5.11E+03*	*5.30E+04*	*2.02E+04*	*3.70E+06*	7.75E+01	*5.48E+01*	*4.21E+03*	1.24E+02

NOTE.—Table 8 is also available in machine-readable form in the electronic edition of the *Astrophysical Journal*.

width can be calculated by using

$$\Gamma_p = 2\,\frac{\hbar^2}{\mu a^2}\,P_l\,C^2S\theta_{\rm sp}^2\,, \tag{19}$$

where P_l is the penetrability of the Coulomb and centrifugal barrier for orbital angular momentum, l, and $a = a_0(A_t^{1/3} + A_p^{1/3})$ is the interaction radius in terms of target (A_t) and projectile (A_p) mass numbers (Iliadis 1997). The dimensionless single-particle reduced width $\theta_{\rm sp}^2$ is given by

$$\theta_{\rm sp}^2 = \frac{a}{2}\,\phi_l^2(a)\,, \tag{20}$$

where $\phi_l^2(a)$ denotes the square of the single-particle radial wave function of the l orbit at the interaction radius a. In the current literature, $\theta_{\rm sp}^2$ in equation (19) is usually set equal to unity. However, as shown in Iliadis (1997), this approximation introduces a significant error in the calculation of Γ_p. The error gives rise to an overestimate of stellar reaction rates if they are influenced by the proton partial width of the compound-nucleus state in question. The two methods for calculating Γ_p discussed above should provide consistent results. For the estimate of proton partial widths we used values of $\theta_{\rm sp}^2$ presented in Iliadis (1997). In terms of R matrix theory (Lane & Thomas 1958), the quantity $\theta_{\rm sp}^2$ in equation (19) represents an "observed" dimensionless single-particle reduced width, rather than a "formal" width. The former quantity is of prime importance for estimating proton partial widths entering the calculation of narrow-resonance strengths.

For stable targets, we used experimental spectroscopic factors from (^{3}He, d) and (d, n) reaction studies in order to estimate proton partial widths of unobserved low-energy resonances. For the estimate of proton partial widths involving short-lived targets, we adopted spectroscopic factors of the mirror states measured in (d, p) reaction studies. This procedure has been tested recently in the sd shell (Iliadis et al. 1999). There it was found that the method of calculating proton partial widths by using equation (19) together with experimental spectroscopic factors provides reliable results on average within a factor of 2.

However, in exceptional cases the experimental spectroscopic factors from the literature have large associated uncertainties. This situation occurs, for example, if the level in question is very weakly populated in a direct single-nucleon transfer reaction or in certain cases in which the single-nucleon transfer can proceed via mixed orbital angular momenta l and $l + 2$. In the former case, a large fraction of the observed particle-spectrum intensity might arise from compound-nucleus or multistep contributions to the reaction. In the latter case, it might be difficult to extract reliably the spectroscopic factor associated with the l-component if the transfer is dominated by the $l + 2$–component. However, because of Coulomb barrier penetrability arguments, the resulting proton partial width

TABLE 9

RECOMMENDED REACTION RATES $N_A\langle\sigma v\rangle_{gs}$ IN cm^3 mol^{-1} s^{-1}

T_9 (GK)	^{36}K(p,γ)	^{37}K(p,γ)	^{38}K(p,γ)	^{39}K(p,γ)	^{39}K(p,α)	^{39}Ca(p,γ)	^{40}Ca(p,γ)*
0.01	...	...	...	...	...	4.91E−53	2.45E−53
0.015.....	...	...	...	...	...	3.05E−45	1.53E−45
0.02	...	...	...	...	...	2.51E−40	1.27E−40
0.03	...	...	...	...	...	3.66E−34	1.86E−34
0.04	...	...	...	...	...	2.93E−30	1.44E−30
0.05	...	...	...	...	...	6.13E−26	8.37E−28
0.06	...	...	...	...	...	3.72E−22	1.07E−25
0.07	...	...	...	...	...	1.84E−19	5.19E−24
0.08	...	...	...	...	...	1.87E−17	1.27E−22
0.09	...	...	...	...	...	6.72E−16	1.89E−21
0.1	...	...	...	...	...	1.15E−14	1.94E−20
0.15	...	...	*1.25E−09*	*2.02E−09*	*4.71E−14*	5.30E−11	7.47E−17
0.2	...	...	*1.81E−07*	*2.56E−07*	*1.42E−11*	3.97E−09	4.09E−13
0.3	...	...	*8.76E−05*	*7.55E−05*	*1.19E−08*	6.26E−07	4.33E−08
0.4	...	...	*3.80E−03*	*2.29E−03*	*7.22E−07*	1.03E−05	1.26E−05
0.5	...	...	*4.84E−02*	*2.38E−02*	*1.30E−05*	5.47E−05	3.52E−04
0.6	...	...	*3.03E−01*	*1.32E−01*	*1.18E−04*	1.60E−04	3.08E−03
0.7	...	...	*1.21E+00*	*4.91E−01*	*6.89E−04*	3.36E−04	1.40E−02
0.8	...	...	*3.59E+00*	*1.38E+00*	*2.96E−03*	*8.30E−04*	4.23E−02
0.9	...	...	*8.61E+00*	*3.19E+00*	*1.02E−02*	*1.73E−03*	9.82E−02
1.0	...	...	*1.77E+01*	*6.32E+00*	*2.97E−02*	*3.17E−03*	1.89E−01
1.5	*4.67E+01*	*5.45E+01*	*1.74E+02*	*5.26E+01*	*1.39E+00*	*2.33E−02*	1.21E+00
2.0	*1.46E+02*	*1.75E+02*	*5.99E+02*	*1.53E+02*	*1.73E+01*	*7.45E−02*	*5.91E+00*
3.0	*4.86E+02*	*6.10E+02*	*2.26E+03*	*4.56E+02*	*5.22E+02*	*3.01E−01*	*3.70E+01*
4.0	*9.18E+02*	*1.21E+03*	*4.70E+03*	*8.83E+02*	*5.55E+03*	*7.27E−01*	*1.11E+02*
5.0	*1.38E+03*	*1.90E+03*	*7.63E+03*	*1.48E+03*	*3.24E+04*	*1.39E+00*	*2.41E+02*
6.0	*1.84E+03*	*2.64E+03*	*1.09E+04*	*2.32E+03*	*1.29E+05*	*2.30E+00*	*4.37E+02*
7.0	*2.29E+03*	*3.40E+03*	*1.45E+04*	*3.31E+03*	*3.52E+05*	*3.48E+00*	*7.02E+02*
8.0	*2.72E+03*	*4.18E+03*	*1.83E+04*	*4.17E+03*	*7.41E+05*	*4.88E+00*	*1.04E+03*
9.0	*3.14E+03*	*4.96E+03*	*2.23E+04*	*4.74E+03*	*1.19E+06*	*6.48E+00*	*1.43E+03*
10.0	*3.54E+03*	*5.72E+03*	*2.64E+04*	*4.98E+03*	*1.48E+06*	*8.21E+00*	*1.87E+03*

NOTE.—Table 9 is also available in machine-readable form in the electronic edition of the *Astrophysical Journal*.

will be most sensitive to the lowest possible l-component. Even in the cases described above, transfer reaction data yield important information for astrophysically interesting levels if significant upper limits can be placed on the spectroscopic factor. Similar arguments hold for known levels in the compound nucleus that have not been observed in transfer reactions. Whenever possible, we estimated upper limits of spectroscopic factors relative to neighboring levels by using published particle spectra obtained from transfer reaction studies. Note that in the literature the estimate $C^2S \leq 1$ is used frequently for levels not populated in transfer reactions. Clearly, the *upper limit* of the proton partial width derived under the latter assumption will be grossly overestimated.

3.4. *Statistical Model Calculations*

With increasing stellar temperature, the Gamow peak, given by equations (7) and (8) for E_0 and Δ, will shift to higher proton bombarding energy. Reaction rates based on resonance energies and strengths are reliable as long as the Gamow peak covers a bombarding energy region that is experimentally well studied. At sufficiently high temperatures, however, an energy regime will be reached that is poorly investigated by experiment. We estimated the maximum temperature, T_{max}, for which the reaction rates are based on experimental resonance energies and strengths from the energy $E_{R,\,max}$ of the highest-lying measured resonance given in Table 2 by using $E_{R,\,max} = E_0(T_{max}) + \Delta(T_{max})$. For stellar temperatures above T_{max} the reaction rates have to be estimated in a different way. Since the level density in the compound nucleus also increases with excitation energy, results obtained by applying the statistical model should in principle provide reliable reaction rates.

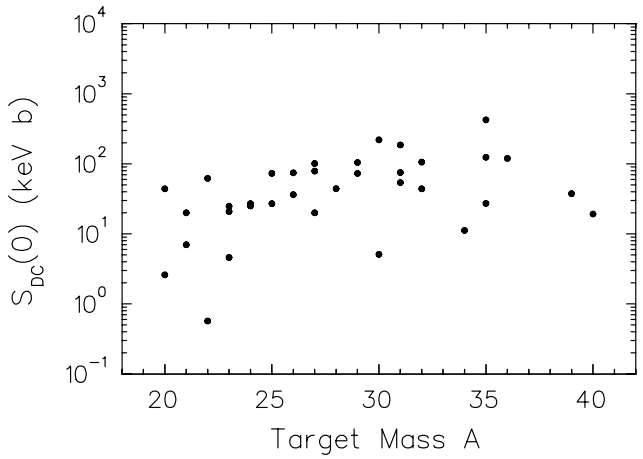

FIG. 1.—Direct proton capture S-factor at zero bombarding energy vs. mass of the target nucleus. The values shown are also listed in column (6) of Table 2.

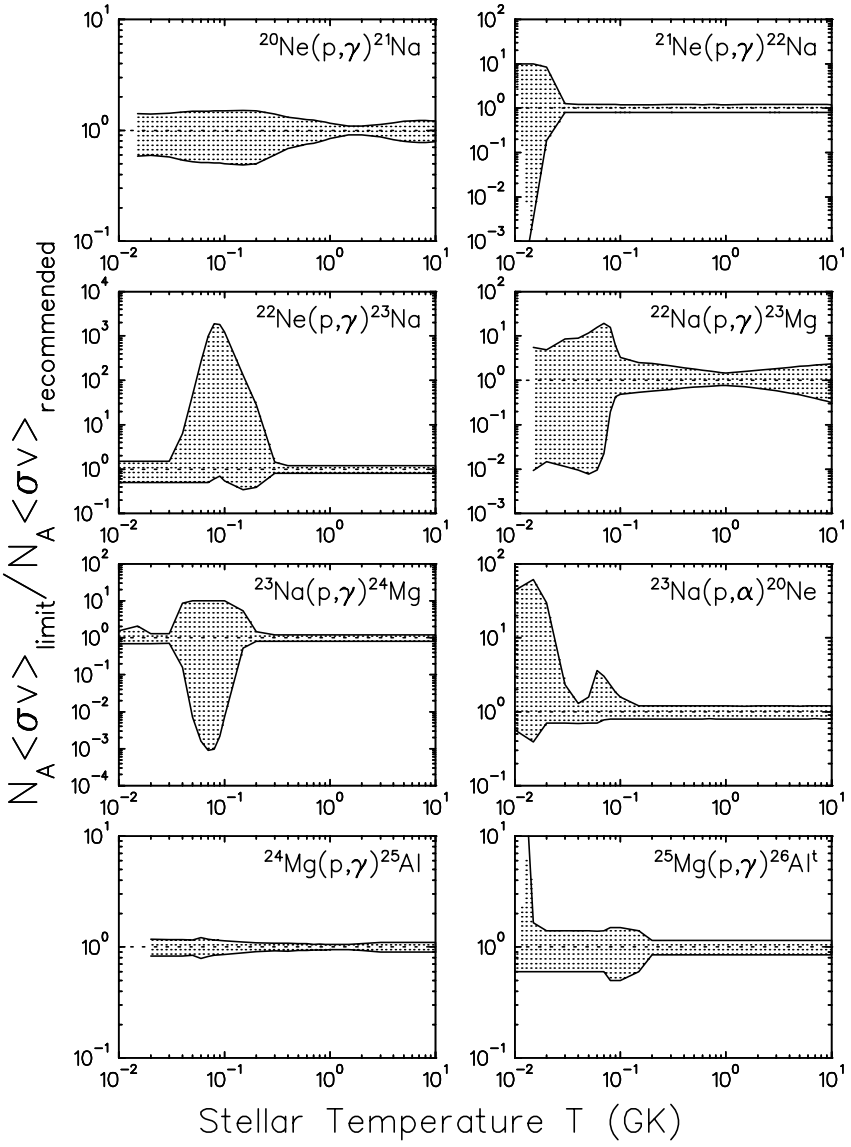

FIG. 2.—Ratios of thermonuclear reaction rates vs. temperature. Solid lines represent upper and lower limits of reaction rates involving stable target nuclei, normalized to our recommended experimental rates (Tables 3–9). Shaded areas indicate the present estimate of reaction rate uncertainties.

Most statistical model calculations for reactions of astrophysical interest are based on the Hauser-Feshbach formalism (Hauser & Feshbach 1952). The theory assumes that there is always a state of appropriate spin and parity available in the compound nucleus through which the reaction can proceed. The most important ingredients for the calculations are transmission coefficients, which are derived from global optical model potentials, and level densities. In the present work, for temperatures above $T_{\max}$ we used the reaction rates presented in the recent compilation by Rauscher & Thielemann (2000), *normalized to our experimental reaction rates at* $T_{\max}$. The results presented by the latter authors are appropriate for thermally populated targets and have been converted to ground-state reaction rates for use in the present work.

At sufficiently low temperatures, the level density in the compound nucleus will be too small for application of the statistical model. Therefore, for each reaction considered, Rauscher & Thielemann (2000) present a lower temperature limit $T_{\rm low}^{\rm HF}$ for the validity of their Hauser-Feshbach reaction rates. However, these estimates are based on level-density arguments alone (see Rauscher, Thielemann, & Kratz 1997), rather than on a rigorous comparison with experimental data. It is evident from the above discussion that the *experimental* reaction rates compiled in the present work can be used to test the reliability of *theoretical* Hauser-Feshbach reaction rates in the mass $A = 20$–40 region. The results of this comparison are presented in § 4.

3.5. *Reaction Rate Uncertainties*

Uncertainties in thermonuclear reaction rates arise from systematic and random errors in the input parameters. Frequently, for example, an unbound state is known to exist near the proton threshold in the compound nucleus, but the corresponding resonance has not been observed. In these cases we have estimated systematic errors by calculating lower and upper limit contributions to the total reaction rates, i.e., by neglecting the resonance, and by estimating a maximum possible contribution (§§ 3.1 and 3.3). Even if energies and strengths are known for all con-

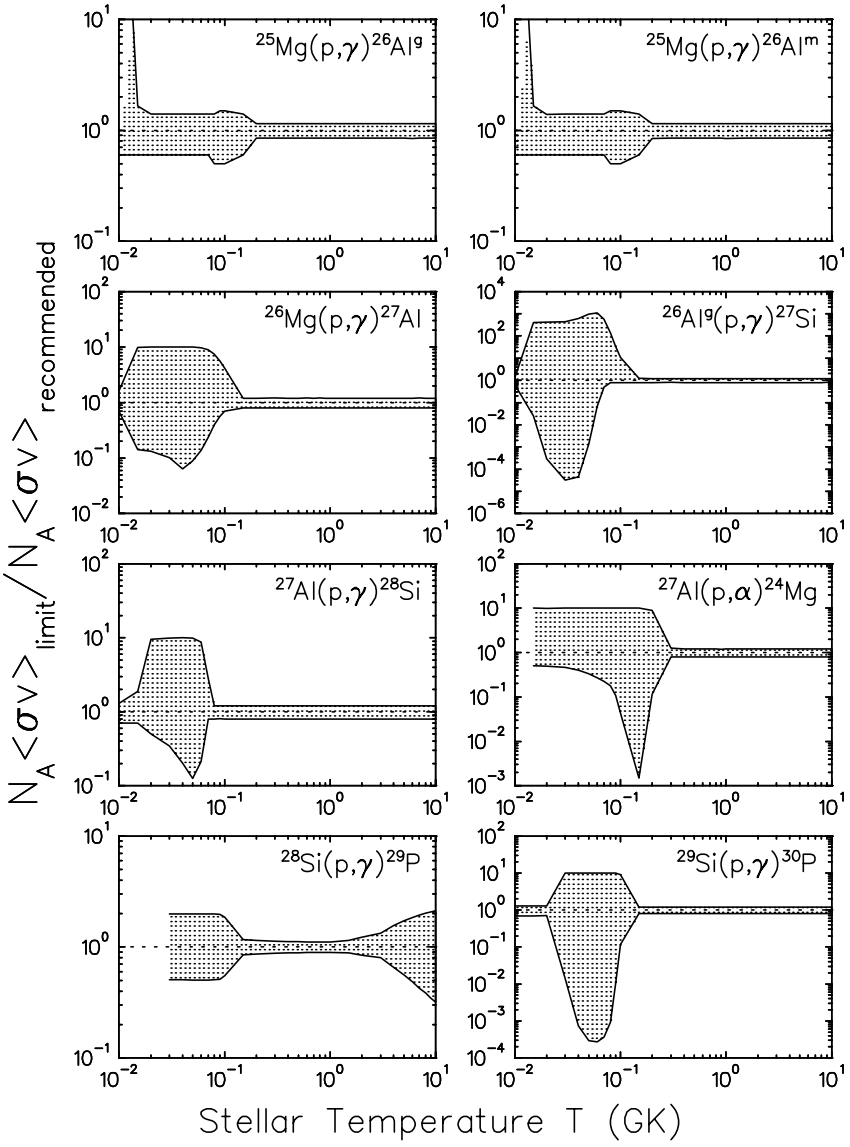

FIG. 3.—Same as Fig. 2

tributing resonances, the total reaction rate will be subject to random errors. For a recent discussion of random error analysis for resonant reaction rates, the reader is referred to Thompson & Iliadis (1999). In the present work, we used this method if estimates of random errors for all input parameters were available (e.g., for ^{24}Mg + p, ^{32}S + p, ^{36}Ar + p, and ^{40}Ca + p). For several reactions, measured resonance strengths are reported in the literature without uncertainties. In these cases, we assumed a typical experimental error of 20% for the reaction rates at the appropriate temperatures. For Hauser-Feshbach reaction rates we adopted the uncertainty of the experimental rate at $T_{\max}$ that was used to normalize the statistical model results (§ 3.4).

It must be emphasized that reaction rates involving short-lived target nuclei have in general larger associated uncertainties compared with stable (or long-lived) target nuclei. The formalism presented in Thompson & Iliadis (1999) is also valid in this case and has been applied, for example, to the reactions ^{27}Si + p, ^{31}S + p, ^{35}Ar + p, and ^{39}Ca + p (Iliadis et al. 1999). However, for several other reactions involving short-lived target nuclei it is difficult to quantify the major source of uncertainty, which is the error in the *predicted* energy of a missing level (§ 3.1). Thus, for reactions involving short-lived target nuclei we do not provide quantitative estimates of reaction rate uncertainties. Qualitative estimates are given in Appendix B.

4. RESULTS

In Table 2 we provide general information on reaction rates compiled in the present work. For each reaction, we list the Q-value (Audi & Wapstra 1995), the reference for the reaction rates, the total number, N_R, of resonances taken into account, the smallest and largest resonance energies, $E_R^{\min}$ and $E_R^{\max}$, and the direct capture S-factor at zero bombarding energy, $S_{\rm DC}(0)$. The latter values are also displayed in Figure 1 versus target mass. For 25 reactions we adopted rates from the literature. In those cases, we reevaluated the reaction rates by using the most recent nuclear structure and reaction information but found only insignificant differences in recommended reaction rates and their associated uncertainties when compared with the previous results. For

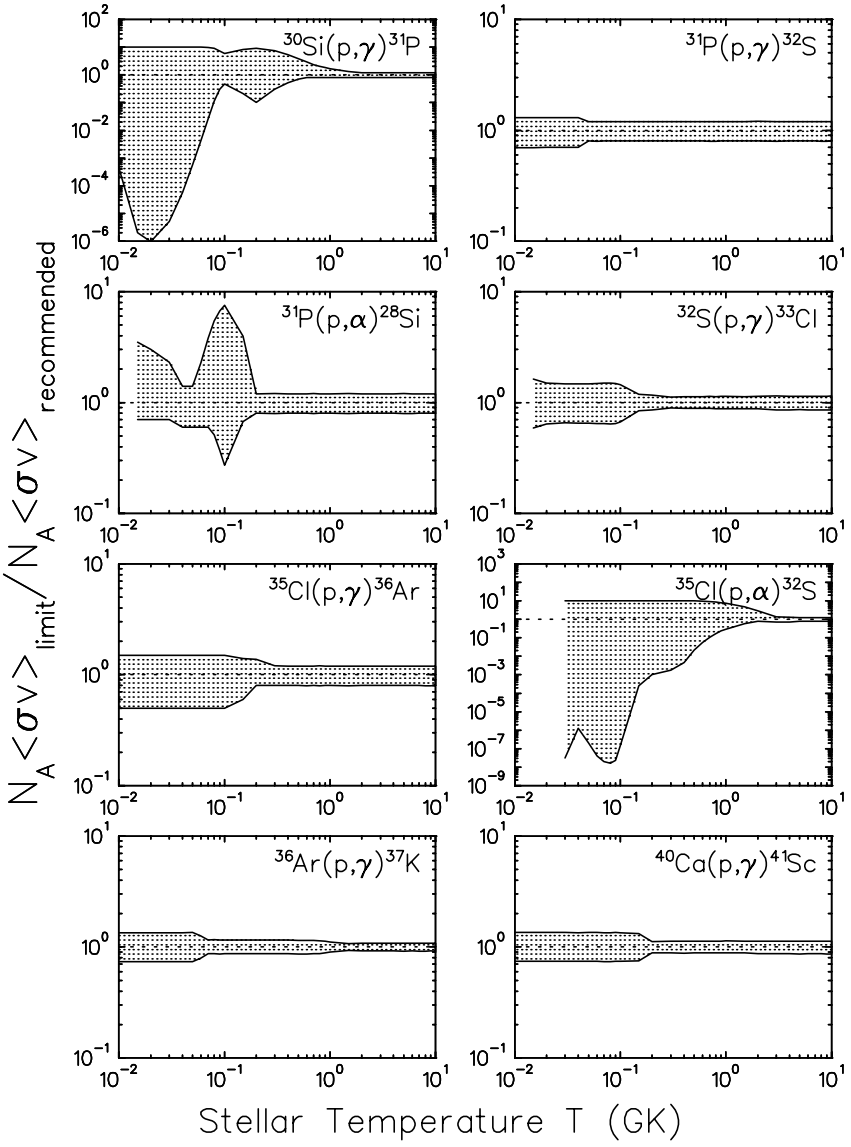

FIG. 4.—Same as Fig. 2

19 other reactions we found significant differences in recommended reaction rates and their associated uncertainties when compared with the previous work. These reactions are labeled "present work" in Table 2 and are discussed in more detail in Appendix B. For the remaining 11 reactions, we recommend statistical model results (Rauscher & Thielemann 2000) for astrophysical calculations.

In Tables 3–9 we present recommended rates for 55 reactions in tabular form on a temperature grid in the range $T = 0.01$–10.0 GK, *assuming that all interacting nuclei are in the ground state*. New reaction rates are labeled with an asterisk. At high temperatures for the majority of reactions we have adopted the results of Hauser-Feshbach calculations, normalized to our experimental reaction rates (see § 3.4). The normalized Hauser-Feshbach reaction rates are represented in the tables by italic numbers. Ellipses are used in the tables if no reaction rate values were reported in the reference given in Table 2 or in cases in which we recommend the use of Hauser-Feshbach results if the temperatures are below the value of $T_{\rm low}^{\rm HF}$ reported by Rauscher & Thielemann (2000).

Lower and upper limits of reaction rates involving stable and long-lived target nuclei are displayed in Figures 2–4. It is apparent that the uncertainties at low stellar temperatures amount to several orders of magnitude for a number of cases, and thus additional experimental work is highly desirable. As noted above, we do not provide quantitative reaction rate error estimates for unstable targets. In the latter case, the reader should be aware that, although the rates are rather well known for certain reactions (see, for example, Iliadis et al. 1999), the uncertainties amount to orders of magnitude for a number of other reactions. Clearly, additional experimental information from future radioactive ion beam studies is essential for improving estimates of thermonuclear reaction rates.

In Figure 5 we display for a number of experimentally well-known reactions (with rate uncertainties less than 25%) the ratio of statistical model reaction rates (from Rauscher & Thielemann 2000) and experimental reaction rates (from the present work) at temperatures between $T_{\rm low}^{\rm HF}$ and $T_{\rm max}$ (see § 3.4). In a few cases, the Hauser-Feshbach reaction rates provide reliable results within a factor of 2.

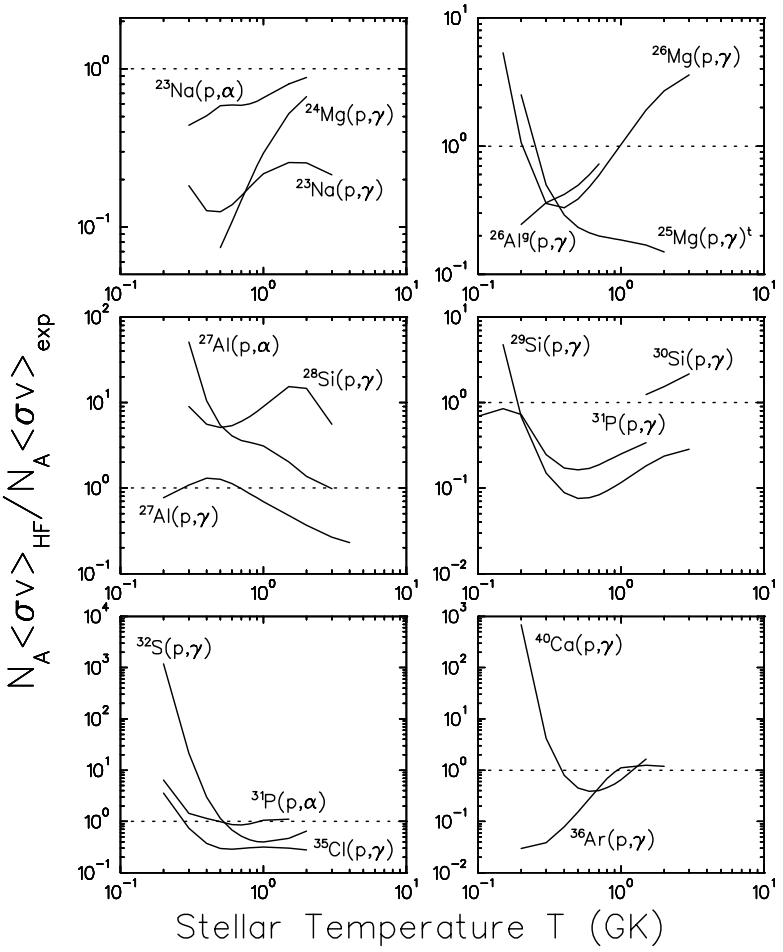

FIG. 5.—Ratios of Hauser-Feshbach reaction rates to our recommended experimental rates (Tables 3–9) at temperatures between T_{low}^{HF} and T_{max} (see § 4). The experimental reaction rates used for the comparison have uncertainties less than 25% (Figs. 2–4).

However, for several other reactions the deviation between theoretical and experimental rates far exceeds the usually quoted "factor of 2 reliability" of statistical model results (Hoffman et al. 1999; Rauscher & Thielemann 2000). Noteworthy are the large discrepancies (up to 3 orders of magnitude) for proton capture reactions on $T_z = 0$ target nuclei ^{24}Mg, ^{32}S, ^{36}Ar, and ^{40}Ca. As mentioned in § 3.4, the lower temperature limit T_{low}^{HF} for the validity of the Hauser-Feshbach reaction rates is based on level-density arguments. Consequently, it appears that this criterion underpredicts the values of T_{low}^{HF} quoted in Rauscher & Thielemann (2000).

5. SUMMARY AND CONCLUSIONS

Proton-induced reaction rates involving stable and unstable target nuclei in the mass region $A = 20$–40 have been evaluated and compiled, assuming that all interacting nuclei are in the ground state. The results are presented in tabular form on a temperature grid in the range $T = 0.01$–10.0 GK. The majority of reaction rates involving stable targets have been normalized by using a standard set of experimental resonance strengths. For unstable targets, reaction rates are estimated by adopting experimental nuclear structure information from corresponding mirror states. For both stable and unstable targets, we have used consistently experimental data obtained from transfer reaction studies. At high stellar temperatures, we adopt the results of theoretical Hauser-Feshbach calculations, *normalized* to our experimental reaction rates. The latter values are represented in Tables 3–9 by italic numbers.

Reaction rate uncertainties are presented and amount to several orders of magnitude for many reactions of astrophysical interest. The smallest overall uncertainties are obtained for the ^{24}Mg$(p,\gamma)^{25}$Al reaction, with experimental errors of 5%–20% over the entire temperature range $T = 0.01$–10.0 GK (Powell et al. 1999). At present, this particular case is the exception rather than the rule. In general, reactions on stable targets have smaller rate uncertainties compared with those on unstable targets. It must be emphasized, however, that for most reactions involving unstable targets with Q-values of a few megaelectron volts, the *number* of low-energy resonances is known since the corresponding mirror nuclei are experimentally well studied. On the other hand, isospin symmetry arguments are not applicable for reactions involving stable targets leading to $T_z = 0$ compound nuclei. In the latter case, one cannot exclude a priori contributions from unobserved low-energy resonances and it is very important to set reliable upper limits on such contributions by carefully measuring transfer reactions.

Our experimental reaction rates have also been used to test recently published Hauser-Feshbach reaction rates in

the mass $A = 20$–40 region. For several reactions, we find deviations far in excess of the usually quoted "factor of 2 reliability" of statistical model results. It appears that part of the discrepancy is caused by underestimation of the lower temperature limit for the validity of Hauser-Feshbach results in Rauscher & Thielemann (2000).

Several of our reaction rates and their corresponding uncertainties deviate from results of previous compilations (Caughlan & Fowler 1988; Angulo et al. 1999). In most cases, the deviations are explained by (1) our adoption of a standard set of absolute resonance strengths in the sd shell, (2) our systematic use of transfer reaction data to estimate contributions of threshold states, and (3) the fact that new experimental information became available recently.

The survey of literature for this review was concluded in 2000 August. Information regarding the calculation of specific reaction rates can be obtained on request from the first author of this paper.

The authors wish to express their gratitude to A. E. Champagne for providing us with data for several reactions prior to publication. This work was supported in part by the Department of Energy under grant DE FG02 97ER41041.

APPENDIX A

EXAMPLES FOR CALCULATING REACTION RATES INVOLVING THERMALLY EXCITED NUCLEI AND REVERSE REACTIONS

At elevated stellar temperatures, excited states of the target nuclei will take part in the nucleosynthesis. Of primary importance for astrophysical model calculations are the reaction rates involving thermally excited nuclei, $N_A\langle\sigma v\rangle^*$, rather than reaction rates involving target nuclei in the ground state, $N_A\langle\sigma v\rangle$. Therefore, the results presented in Tables 3–9 have to be corrected for effects of thermal excitation. The ratio $N_A\langle\sigma v\rangle^*/N_A\langle\sigma v\rangle$ has been estimated previously by using a statistical model (Angulo et al. 1999; Rauscher & Thielemann 2000).

For a reaction $a + b \rightleftharpoons c + d$ involving nonidentical particles, the forward and reverse rates are related by

$$\frac{N_A\langle\sigma v\rangle^*_{cd\to ab}}{N_A\langle\sigma v\rangle^*_{ab\to cd}} = \frac{(2J_a+1)(2J_b+1)}{(2J_c+1)(2J_d+1)}\left(\frac{G_a G_b}{G_c G_d}\right)\left(\frac{A_a A_b}{A_c A_d}\right)^{3/2} e^{-11.605Q/T_9}\,, \tag{A1}$$

where J and A are the spins and masses (in atomic mass units) of the participating nuclei, and Q is the reaction Q-value (in megaelectron volts) for the forward reaction (Fowler et al. 1967). The temperature-dependent normalized partition functions are

$$G_i = \sum_\mu \frac{2J_{i\mu}+1}{2J_{i0}+1}\, e^{-E_{i\mu}/kT}\,, \tag{A2}$$

where $J_{i\mu}$ and $E_{i\mu}$ are, respectively, the spin and excitation energy of state μ in nucleus i and J_{i0} is the ground-state spin of nucleus i. Tabulated values of G_i are presented in Angulo et al. (1999) and Rauscher & Thielemann (2000). For a capture reaction $a + b \rightleftharpoons c + \gamma$, forward and reverse rates are related by

$$\frac{\lambda^*_{c\gamma\to ab}}{N_A\langle\sigma v\rangle^*_{ab\to c\gamma}} = 9.8685\times 10^9 T_9^{3/2}\,\frac{(2J_a+1)(2J_b+1)}{2J_c+1}\,\frac{G_a G_b}{G_c}\left(\frac{A_a A_b}{A_c}\right)^{3/2} e^{-11.605Q/T_9}\,, \tag{A3}$$

where λ is the photodisintegration rate per second and Q is in megaelectron volts (Fowler et al. 1967).

As a first example, consider the reaction ^{23}Na$(p,\alpha)^{20}$Ne at a stellar temperature of $T = 0.6$ GK. Assuming that the ^{23}Na target nuclei are in the ground state, from Table 3 we obtain for the reaction rate $N_A\langle\sigma v\rangle = 4.10\times 10^2$ cm^3 mol^{-1} s^{-1}. At this relatively low temperature, the rate for thermally excited ^{23}Na target nuclei is given by $N_A\langle\sigma v\rangle^* = N_A\langle\sigma v\rangle$ (see, for example, Rauscher & Thielemann 2000). The corresponding reverse reaction rate is obtained from equation (A1) with $J(^{23}\mathrm{Na}) = 3/2$, $J(^{20}\mathrm{Ne}) = 0$, $J(p) = 1/2$, $J(\alpha) = 0$, and $Q_{p\alpha} = 2.3765$ MeV. The result for $^{20}\mathrm{Ne} + \alpha \to {}^{23}\mathrm{Na} + p$ is $N_A\langle\sigma\mathrm{v}\rangle^* = 5.51\times 10^{-18}$ cm^3 mol^{-1} s^{-1}. At this temperature, the partition functions G_i are equal to unity (Rauscher & Thielemann 2000).

As a second example, consider the reaction $^{32}\mathrm{S}(p,\gamma)^{33}$Cl at a stellar temperature of $T = 10$ GK. Assuming that the ^{32}S target nuclei are in the ground state, from Table 7 we obtain for the reaction rate the value $N_A\langle\sigma\mathrm{v}\rangle = 1.05\times 10^4$ cm^3 mol^{-1} s^{-1}. The rate for thermally excited ^{32}S target nuclei can be obtained by multiplying this value with a "stellar enhancement factor" of 0.83 (Rauscher & Thielemann 2000) with the result $N_A\langle\sigma\mathrm{v}\rangle^* = 8.72\times 10^3$ cm^3 mol^{-1} s^{-1}. The corresponding reverse reaction rate (i.e., the photodisintegration of ^{33}Cl) is obtained from equation (A3) with $J(^{32}\mathrm{S}) = 0$, $J\ (p) = 1/2$, $J(^{33}\mathrm{Cl}) = 3/2$, and $Q_{p\gamma} = 2.2765$ MeV. Adopting the values $\mathrm{G}(^{32}\mathrm{S}) = 1.6$, $\mathrm{G}(p) = 1$, and $\mathrm{G}(^{33}\mathrm{Cl}) = 1.9$ from Rauscher & Thielemann (2000), one obtains for $\gamma + {}^{33}\mathrm{Cl} \to p + {}^{32}\mathrm{S}$ the result $\lambda^* = 7.79\times 10^{13}$ s^{-1}.

APPENDIX B

NUCLEAR PHYSICS INPUT

This appendix gives details of the nuclear physics properties used as input to the reaction rate calculations. Only those reactions are discussed here that are labeled "present work" in Table 2. Information on individual proton threshold states that have not been observed as resonances in proton-induced reactions is presented in Table 10.

TABLE 10

SUMMARY OF PARAMETERS FOR PROTON THRESHOLD STATES NOT OBSERVED AS RESONANCES IN (p,γ) AND (p,α) REACTIONS

E_x (keV) (1)	E_R^{cm} (keV) (2)	J_n^π (3)	C^2S (4)	l_R (5)	Γ_p (eV) (6)	Γ_γ (eV) (7)	$\omega\gamma$ (eV) (8)
^{21}Ne(p,γ):							
6756 *6*	16.6		≤ 1	0	$\leq 1.0 \times 10^{-23}$		$\leq 6.2 \times 10^{-24}$
6834 *7*[a]	94.6	$(0, 1)^+$	≤ 0.02[b]	2	$\leq 5.1 \times 10^{-9}$		$\leq 6.4 \times 10^{-10}$
^{25}Mg(p,γ):							
6343.46 *8*	36.9	(4^-)	0.0047, 0.006[c]	1, 3	$\leq 3.2 \times 10^{-20}$		$\leq 2.4 \times 10^{-20}$
6363.99 *8*	57.4	3^+	$0.07+0.13$	$0+2$	4.8×10^{-13}		2.8×10^{-13}
6398.64 *21*	92.1	2^-	$0.007+0.010$	$1+3$	2.8×10^{-10}		1.2×10^{-10}
6414.46 *10*	107.9	0^+	0.015	2	2.5×10^{-10}		2.1×10^{-11}
6436.44 *11*	129.9	5^+	0.0007, 0.0031[c]	2, 4	$\leq 1.6 \times 10^{-10}$		$\leq 1.5 \times 10^{-10}$
^{26}Mg(p,γ):							
8287 *1*	15.7	$9/2^-$	≤ 1	5	$\leq 3.4 \times 10^{-40}$		$\leq 1.7 \times 10^{-39}$
8324 *1*	52.7	5/2	0.017[d]	(2)[e]	$\leq 7.4 \times 10^{-17}$		$\leq 2.2 \times 10^{-16}$
8361 *3*	89.7		0.0017[d]	(0)[e]	$\leq 2.0 \times 10^{-10}$		$\leq 2.0 \times 10^{-10}$
8376 *1*	104.7		0.0022[d]	(1)[e]	$\leq 9.9 \times 10^{-10}$		$\leq 9.9 \times 10^{-10}$
8396 *1*	124.7	11/2	≤ 1	(5)[e]	$\leq 1.4 \times 10^{-13}$		$\leq 8.6 \times 10^{-13}$
8408 *3*	136.7						$\leq 3.0 \times 10^{-8}$[f]
^{27}Al(p,γ):							
11656.6 *5*	71.7	2^+	$\leq 0.0017+0.017$[g]	$0+2$	$\leq 7.8 \times 10^{-14}$	≈ 0.035[h]	$\leq 6.5 \times 10^{-15}$
11669.4 *4*	84.5	1^-	≤ 0.0063[g]	1	$\leq 2.6 \times 10^{-12}$	≈ 0.28[h]	$\leq 3.9 \times 10^{-13}$
^{29}Si(p,γ):							
5701.7 *4*	107.2	1^+	≤ 0.003[i]	0	$\leq 5.1 \times 10^{-11}$	4.1×10^{-2}[k]	$\leq 3.8 \times 10^{-11}$
5714 *3*	119.5	$(5, 7)^+$	≤ 0.01[i]	4	$\leq 3.6 \times 10^{-15}$		$\leq 9.9 \times 10^{-15}$
5808 *3*	213.5	$(3, 5)^+$	≤ 0.009[j]	2	$\leq 1.8 \times 10^{-7}$		$\leq 3.1 \times 10^{-7}$
^{30}Si(p,γ):							
7314 *4*	16.9	$(5/2, 7/2)^-$	0.002[l]	3	1.0×10^{-42}		3.0×10^{-42}
7349 *5*	51.9	$(3/2, 5/2)^-$	≤ 1	1	$\leq 5.3 \times 10^{-17}$		$\leq 1.1 \times 10^{-16}$
7441.2 *7*	144.1	$11/2^+$	≤ 1	6	$\leq 1.4 \times 10^{-16}$		$\leq 8.4 \times 10^{-16}$
7466 *2*	168.9	$(7/2, 9/2)^-$	≤ 0.003[m]	3	$\leq 2.9 \times 10^{-11}$		$\leq 1.2 \times 10^{-10}$
7715 *5*	417.9		≤ 0.02[m]	0	≤ 0.24		$\leq 2.4 \times 10^{-1}$
7736 *4*	438.9	$(5/2, 7/2)^-$	0.02[l]	3	9.3×10^{-5}		2.8×10^{-4}

B1. THE ^{21}Ne$(p,\gamma)^{22}$Na REACTION

The contributions of 46 resonances for $E_R^{cm} = 17$–1937 keV were taken into account. Resonances were measured for $E_R^{cm} \geq 121$ keV, and the corresponding experimental energies and strengths have been adopted from Endt (1990, 1998) and references therein. Two threshold states, corresponding to resonance energies of $E_R^{cm} = 17$ and 95 keV, have been considered. The former state, which was neglected in Angulo et al. (1999), might influence the total rates at $T \leq 0.02$ GK. For the state corresponding to $E_R^{cm} = 95$ keV, we estimated an upper limit of $C^2S \leq 0.02$ from the ^{21}Ne(d,p) work of Neogy, Middleton, & Scholz (1972). The rate uncertainty due to this resonance is negligible, in agreement with the conclusions in El Eid & Champagne (1995) but in disagreement with Angulo et al. (1999), who assumed $C^2S \leq 1$. The direct capture S-factor was adopted from Rolfs, Sharpiro, & Winkler (1975). At $T \geq 0.05$ GK, our total rate is in agreement with Angulo et al. (1999) but disagrees up to a factor of 300 at $T \geq 0.02$ GK, mainly because of differences in the adopted strength estimates for the threshold states. Below $T = 0.02$ GK, our total rate is uncertain by several orders of magnitude.

B2. THE ^{25}Mg$(p,\gamma)^{26}$Al REACTION

The contributions of 81 resonances for $E_R^{cm} = 37$–1762 keV were considered. Resonances were measured for $E_R^{cm} \geq 189$ keV. The measured strengths, adopted from Endt (1990, 1998) and references therein, have been normalized by using the absolute $\omega\gamma$ standards listed in Table 1. The contributions of five threshold states have been taken into account. The corresponding $\omega\gamma$ values were adopted from Iliadis et al. (1996). The direct capture contribution (from Endt & Rolfs 1987) is negligible. The total reaction rate has been multiplied by the ground-state branching ratio f_0 and by $1 - f_0$ in order to estimate the reaction rates for populating the ground and isomeric states in ^{26}Al, respectively. Values of f_0 were adopted from Endt & Rolfs (1987) and Iliadis et al. (1996). Our recommended total rates are larger than the results of Angulo et al. (1999) at $T \leq 0.04$ by 20%–40%, presumably because of small differences in adopted resonance energies of the threshold states, but the observed deviations are within the quoted reaction rate uncertainties. However, above $T = 3$ GK our results are smaller up to factors of 3–4 compared with Angulo et al. (1999) because of differences in the adopted Hauser-Feshbach reaction rates. Our total reaction rates are uncertain by about a factor of 2 at $T \approx 0.1$ GK, with smaller (larger) uncertainties above (below) $T = 0.2$ GK ($T = 0.02$ GK). Note that the value $J^\pi = 4^-$ for $E_R^{cm} = 130$ keV quoted in Angulo et al. (1999) should be replaced by the correct assignment, $J^\pi = 5^+$ (see Iliadis et al. 1996).

TABLE 10—*Continued*

E_x (keV) (1)	E_R^{cm} (keV) (2)	J_n^π (3)	C^2S (4)	l_R (5)	Γ_p (eV) (6)	Γ_γ (eV) (7)	$\omega\gamma$ (eV) (8)
^{29}P(p,γ):							
(4733)[n]	333.0	(3_1^+)	0.04[o]	2	9.1×10^{-5}	4.9×10^{-3}	1.5×10^{-4}
(4888)[n]	488.0	(2_3^+)	0.11[o]	2	2.2×10^{-2}	4.2×10^{-3}	4.4×10^{-3}
5145 *10*	745.0	(3_2^+)	0.02[p]	2	2.4×10^{-1}	8.2×10^{-3}	1.4×10^{-2}
5288 *10*	888.0	(3_1^-)	0.36[o]	3	7.5×10^{-1}	9.4×10^{-3}	1.6×10^{-2}
6117 *10*	1717.0	(1_1^-)	0.28[o]	1	1.9×10^{4}	8.2×10^{-1}	6.1×10^{-1}
6233 *10*	1833.0	(4_1^-)	0.35[o]	3	1.9×10^{2}	2.9×10^{-3}	6.5×10^{-3}
^{31}P(p,γ):							
$\approx$9023[q]	$\approx$160.0		0.026[r]	3	1.4×10^{-11}		1.8×10^{-11}[s]
^{30}S(p,γ):							
(620 ± 70)[t]	330.0	$(1/2_1^+)$	0.22[u]	0	1.3×10^{-2}	4.8×10^{-4}	4.6×10^{-4}
($\approx$1400)[v]	1109.0	$(5/2_1^+)$	0.02[u]	2	3.6×10^{0}	4.0×10^{-4}	1.2×10^{-3}
^{32}S(p,γ):							
2351.8 *0.3*	75.3	$3/2^+$	0.07[w]	2	4.9×10^{-18}	6.6×10^{-3}[x]	1.0×10^{-17}
^{35}Cl(p,γ):							
8555.5 *6*	49.6	2^+	0.034[y]	0	9.6×10^{-24}		6.0×10^{-24}[aa]
8672 *3*	166.1	$\leq 4^+$			9.0×10^{-10}[z]		4.5×10^{-10}[aa]
^{35}K(p,γ):							
(3260)[bb]	700.0	(2_1^+)	$0.009 + 0.01$[u]	$0+2$	1.9×10^{-1}	6.0×10^{-3}	3.6×10^{-3}

[a] Most likely assignment is $J^\pi = 0^+$ (Endt 1998), with $E_x = 6235$ keV in ^{22}Ne as mirror state.
[b] Estimate from Fig. 1 and Table 1 in Neogy et al. 1972.
[c] Angular distributions in ^{25}Mg(^{3}He, d) do not allow reliable extraction of individual l components; results are presented for pure transfers l and $l + 2$ (see Iliadis et al. 1996).
[d] From a recent reanalysis of ^{26}Mg(^{3}He, d)^{27}Al stripping data (C. Rowland 2000, private communication).
[e] Only the lowest possible l—value is listed here.
[f] Experimental upper limit (Buchmann et al. 1980).
[g] From present reanalysis of ^{27}Al(^{3}He, d)^{28}Si stripping data of Champagne et al. 1986.
[h] Estimated by using measured values of $\omega\gamma_{\alpha\gamma}$ (Endt & van der Leun 1978), Γ_α/Γ (Champagne et al. 1988), and Γ_p of column 6; the same estimate also yields values of $\Gamma_\alpha \approx 0.14$ and 0.18 eV for the resonances at $E_R^{cm} = 72$ and 85 keV, implying ^{27}Al(p,α) resonance strengths of $\omega\gamma \leq 2.6 \times 10^{-14}$ and 2.6×10^{-13} eV, respectively.
[i] Estimate from Fig. 2 and Table 2 in Dykoski & Dehnhard 1976.
[j] From Dykoski & Dehnhard 1976.
[k] Estimated from experimental mean lifetime (Endt 1998).
[l] From ^{30}Si(^{3}He, d)P^{31}P transfer study of Vernotte et al. 1990.
[m] Estimated from Fig. 1 and Table 1 of Vernotte et al. 1990.
[n] Excitation energies estimated by using the isobaric multiplet mass equation; the errors are about ± 40 keV (see text).
[o] Spectroscopic factors of mirror states, measured in ^{29}Si(d, p) work of Mackh et al. 1973.
[p] Estimate from Figs. 5 and 7 of Mackh et al. 1973.
[q] Doublet of states at $E_x = 9023 \pm 2$ and 9024 ± 2 keV with $J^\pi = 3^-$ and 6^- (4^-), respectively; only the total contribution is given here.
[r] From Kalifa et al. 1978.
[s] Estimated by using $\Gamma_\gamma/\Gamma = 0.75 \pm 0.19$ (Ross et al. 1995); the measured value $\Gamma_\alpha/\Gamma = 0.37 \pm 0.13$ (Ross et al. 1995) for $E_x = 9023$ keV yields $\omega\gamma_{p\alpha} = 9.1 \times 10^{-12}$ eV.
[t] Estimated by using the isobaric multiplet mass equation (see text).
[u] From shell model calculation (Herndl et al. 1995).
[v] Estimated from Fig. 4 of Benenson et al. 1977.
[w] Average of $C^2S(d, n) = 0.07$ (Elbakr et al. 1972), $C^2S(^3\text{He}, d) = 0.061$ (Inglima et al. 1975), and $C^2S(d, p) = 0.07$ (Mermaz et al. 1971).
[x] From measured lifetime, assuming $\Gamma \approx \Gamma_\gamma$.
[y] From Iliadis et al. 1994.
[z] See discussion in text.
[aa] Estimated by using Γ_γ/Γ from Ross et al. 1995; the measured upper limits of Γ_α/Γ (Ross et al. 1995) for $E_x = 8556$ and 8672 keV yield $\omega\gamma_{p\alpha} \leq 4.1 \times 10^{-25}$ and $\leq 5.4 \times 10^{-11}$ eV.
[bb] Estimated by using Coulomb displacement energy calculations (Herndl et al. 1995).

B3. THE ^{26}MG(p, γ)^{27}AL REACTION

A total of 133 resonances for $E_R^{cm} = 16$–2867 keV has been considered. Resonances were measured for $E_R^{cm} \geq 149$ keV, and the measured strengths, adopted from Endt (1990) and references therein, have been normalized by using the absolute $\omega\gamma$ standards listed in Table 1. The contributions of six threshold states were taken into account. The corresponding resonance strengths have been estimated by using spectroscopic factors from a recent reanalysis of ^{26}Mg (^{3}He, d)^{27}Al stripping data (C. Rowland 2000, private communication). The direct capture contribution, adopted from Iliadis et al. 1990, is important only at $T \leq 0.01$ GK. Our recommended total rates deviate from the results of Angulo et al. (1999) by about a factor of 2 above $T = 0.02$ GK, since we adopt absolute $\omega\gamma$ values from Table 1 and we use different spectroscopic factors for the threshold states. Our total reaction rates are uncertain by about 20% above $T = 0.2$ GK. Below this temperature, the uncertainties amount to as much as a factor of 15.

B4. THE ^{27}Al$(p, \gamma)^{28}$Si REACTION

A total of 105 resonances in the region $E_R^{cm} = 72$–3819 keV was taken into account. Resonances were measured for $E_R^{cm} \geq 195$ keV. Measured strengths have been adopted from Endt (1990) and Chronidou et al. (1999) and were normalized by using the absolute $\omega\gamma$ values of Table 1. The contributions of four threshold states have been taken into account. The estimated resonance parameters of only the two most important states, corresponding to $E_R^{cm} = 72$ and 85 keV, are listed in Table 10. Spectroscopic factors have been adopted from the present reanalysis of ^{27}Al(^{3}He, d)^{28}Si stripping data of Champagne et al. (1986). For $E_R^{cm} = 72$ keV, the measured deuteron angular distribution implies a dominant $l = 2$ contribution. However, a small $l = 0$ contribution cannot be excluded and has been taken into account in the present rate estimate. Note that our value of $C^2S(l = 2)$ listed in Table 10 deviates from the result quoted in Champagne et al. (1986) by factors of 2–3. For $E_R^{cm} = 85$ keV, the measured deuteron angular distribution can be described either by a pure $l = 1$ or $l = 3$ transfer. The upper limit contribution of this resonance has been estimated assuming a pure $l = 1$ transfer, whereas a pure $l = 3$ transfer was assumed in Champagne et al. (1986). The direct capture contribution has been recalculated in the present work (Table 2) and found to be larger by about 50% when compared with the result of Timmermann et al. (1988). However, the direct capture process is important only at temperatures $T \leq 0.015$ GK. Our recommended total rates deviate from the results of Angulo et al. (1999) up to a factor of 20 below $T = 0.07$ GK, mainly because improved estimates of spectroscopic factors for the threshold states have been used in the present work. At temperatures $T = 0.07$–6.0, the present results agree with Angulo et al. (1999). At higher temperatures, our results are smaller by factors of 2–3, presumably due to differences in the adopted Hauser-Feshbach reaction rates. Our total reaction rates are uncertain by about 20% above $T = 0.1$ GK. Below this temperature, the uncertainties are up to 1 order of magnitude.

B5. THE ^{27}Al$(p, \alpha)^{24}$Mg REACTION

A total of 90 resonances in the region $E_R^{cm} = 72$–2967 keV was taken into account. Resonances were measured for $E_R^{cm} \geq 486$ keV, and the measured strengths have been adopted from Endt (1998). The contributions of eight natural parity states close to the proton threshold were taken into account. The corresponding resonance strengths have been estimated from measurements of $\omega\gamma_{\alpha\gamma}$ (Endt & van der Leun 1978), Γ_α/Γ and Γ_p/Γ (Champagne et al. 1988), and Γ_p. The latter values were obtained from a present reanalysis of ^{27}Al(^{3}He, d)^{28}Si stripping data (Champagne et al. 1986). Only the estimates of (p, α) resonance strengths for two states, corresponding to $E_R^{cm} = 72$ and 85 keV, are listed in Table 10. Low-energy wings of broad resonances are negligible above $T = 0.01$ GK. Our recommended total rates deviate from the results of Angulo et al. (1999) up to a factor of 10 below $T = 0.09$ GK, mainly because improved estimates of spectroscopic factors for the threshold states are used here. Above $T = 0.15$ GK, the present results are in approximate agreement with Angulo et al. (1999). Our total reaction rates are uncertain by about 20% above $T = 0.3$ GK. Below this temperature, the uncertainties amount to as much as 3 orders of magnitude.

B6. THE ^{29}Si$(p, \gamma)^{30}$P REACTION

A total of 79 resonances in the region $E_R^{cm} = 107$–3076 keV was considered. Resonances were measured for $E_R^{cm} \geq 313$ keV, and the measured strengths have been adopted from Endt (1998) and references therein. The $\omega\gamma$ values were normalized by using $S_{p\gamma}(E_R = 416 \text{ keV}) = 0.88 \pm 0.10$ eV from Table 1 in Sargood (1982). The contributions of three threshold states were taken into account. Spectroscopic factors were adopted from Table 2 of Dykoski & Dehnhard (1976) or have been estimated from their Figure 2. The direct capture contribution has been calculated in the present work and dominates the reaction rates only below $T = 0.03$ GK. Our recommended total rates agree with the results of Caughlan & Fowler (1988) at temperatures $T = 0.15$–5.0 GK. However, between $T = 0.03$–0.1 GK the deviations in the total reaction rates amount to up to 3 orders of magnitude. Better agreement within a factor of 2 is obtained below $T = 0.03$ GK. Thus, it appears likely that at low temperatures the reaction rate contribution of threshold states was entirely neglected in Caughlan & Fowler (1988). Above $T = 6.0$ GK the deviations amount to a factor of about 2, presumably due to differences in the adopted Hauser-Feshbach reaction rates. Our total reaction rates are uncertain by about 20% above $T = 0.15$ GK. Below this temperature, the uncertainties are up to 3–4 orders of magnitude.

B7. THE ^{30}Si$(p, \gamma)^{31}$P REACTION

A total of 98 resonances in the region $E_R^{cm} = 52$–2929 keV was considered. Resonances were measured for $E_R^{cm} = 483$ keV and the measured strengths, adopted from Endt (1990) and references therein, were normalized by using the absolute $\omega\gamma$ values listed in Table 1. The contributions of six threshold states have been taken into account. Spectroscopic factors were adopted from Table 1 of Vernotte et al. (1990) or have been estimated from their Figure 1. The direct capture contribution has been calculated in the present work and dominates the lower limit of the reaction rates at $T \leq 0.15$ GK. Above $T = 0.2$ GK, our recommended total rates agree with the results of Caughlan & Fowler (1988) within a factor of 2–3. Below $T = 0.15$ GK the deviations amount to up to several orders of magnitude. It appears likely that the reaction rate contribution of threshold states was entirely neglected in Caughlan & Fowler (1988). Our total reaction rates are uncertain by about 30% above $T = 1.0$ GK. Below this temperature, the uncertainties amount to as much as 6 orders of magnitude.

B8. THE ^{29}P$(p, \gamma)^{30}$S REACTION

A total of six states corresponding to $E_R^{cm} = 333$–1833 keV has been taken into account and their parameters are given in Table 10. The contributions of seven additional states (not listed in Table 10) were also estimated but were found to be negligible. The excitation energies of four threshold states in ^{30}S have been adopted from the ^{28}Si(^{3}He, np) work of Yokata et al. (1982). The excitation energies corresponding to the two lowest-lying resonances have not been measured and their values

have been estimated (see Iliadis 1999) by using the isobaric multiplet mass equation, IMME. For nine isospin triplet states in the $A = 30$ system the analog assignments are unambiguous. In these cases, the IMME reproduces the experimental ^{30}S excitation energies on average within 40 keV. Therefore, the present excitation energy estimates are more reliable than the previous results of Wiescher & Görres (1988), who performed Thomas-Ehrman shift calculations. Spectroscopic factors have been adopted from the mirror states, measured in the ^{29}Si$(d, p)^{30}$Si work of Mackh et al. (1973). Gamma-ray partial widths were estimated by using measured lifetimes of ^{30}Si mirror levels. The direct capture contribution has been calculated in the present work and dominates the reaction rates at $T \leq 0.1$ GK. Our recommended total rate agrees with the results of Wiescher & Görres (1988) at temperatures $T \leq 0.06$ GK and $T \leq 0.9$ GK. However, at $T = 0.07$–0.8 GK the deviations amount to as much as 3 orders of magnitude. Our total reaction rates are uncertain below $T = 1.0$ GK by orders of magnitude, mainly because of uncertainties in the excitation energies of two unobserved ^{30}S levels corresponding to resonances at $E_R^{cm} = 333$ and 488 keV.

B9. THE ^{31}P$(p, \gamma)^{32}$S REACTION

A total of 42 resonances in the region $E_R^{cm} = 160$–1963 keV was taken into account. Resonances were measured for $E_R^{cm} = 195$ keV. Measured strengths have been adopted from Endt (1990, 1998) and references therein and were normalized by using the absolute $\omega\gamma$ values of Table 1. Two states near the proton threshold have been taken into account but only their total contribution is listed in Table 10. The total $\omega\gamma$ value of the doublet is estimated by using the spectroscopic factor reported in the ^{31}P$(^3$He$, d)^{32}$S stripping work of Kalifa et al. (1978) and the measured value of Γ_γ/Γ (Ross et al. 1995). Note that the state at $E_x = 9196$ keV reported in Endt (1990) has been omitted in the present analysis, since Endt (1998) considers it to be identical to the $E_x = 9208$ keV level. The direct capture S-factor has been adopted from Iliadis et al. (1993a). Our total reaction rates are uncertain by about 20% (30%) above (below) $T = 0.05$ GK.

B10. THE ^{31}P$(p, \alpha)^{28}$Si REACTION

A total of 25 resonances in the region $E_R^{cm} = 160$–1963 keV was taken into account. Resonances were measured for $E_R^{cm} \geq 372$ keV. Measured strengths have been adopted from Endt (1990, 1998) and references therein. The contributions of four natural parity states close to the proton threshold were taken into account. The corresponding resonance strengths have been estimated from measurements of $\omega\gamma_{p\gamma}$ (Endt 1998), Γ_α/Γ and Γ_γ/Γ (Ross et al. 1995), and Γ_p. The latter values were calculated from spectroscopic factors reported in Kalifa et al. (1978) or have been estimated from their Figure 1. Only the (p, α) resonance strength corresponding to the level at $E_x = 9023$ keV is given in Table 10. Contributions of low-energy wings of broad resonances and high-energy wings of subthreshold states have been adopted from Iliadis et al. (1993a). At $T \geq 0.2$ GK, our total reaction rates are uncertain by about 20%. Below this temperature, the uncertainties amount to up to 1 order of magnitude.

B11. THE ^{30}S$(p, \gamma)^{31}$Cl REACTION

Two states corresponding to $E_R^{cm} = 330$ and 1109 keV were taken into account and their parameters are given in Table 10. Both states are expected to occur below the lowest-lying observed ^{31}Cl level at $E_x = 1820$ keV (Endt 1998). The location of the first ^{31}Cl state has been estimated by using the IMME (see Iliadis et al. 1999), since the other members of the J^π, $T = 1/2^+$, 3/2 isospin quartet in ^{31}Si, ^{31}P, and ^{31}S are known experimentally (Endt 1998). This procedure yields a value of $E_x = 620 \pm 70$ keV, which is more reliable when compared with the result of Herndl et al. (1995), who performed Coulomb displacement energy calculations. For the corresponding resonance energy one obtains $E_R^{cm} = 330 \pm 45$ keV, calculated directly from the mass excess values rather than by using the relation $E_R^{cm} = E_x - Q_{p\gamma}$. The energy of the $5/2^+$ level has been estimated from Figure 4 of Benenson et al. (1977), which shows a weak peak at $E_x \approx 1400$ keV. Shell model spectroscopic factors were adopted from Herndl et al. (1995). Gamma-ray partial widths have been estimated by using measured lifetimes of ^{31}Si mirror levels. The direct capture contribution was also adopted from Herndl et al. (1995). Our recommended total rate agrees with the results of Herndl et al. (1995) at temperatures $T \leq 0.07$ and $T \geq 1.5$ GK. However, at $T = 0.08$–1.0 GK the deviations amount to up to 5 orders of magnitude. Our total reaction rates are uncertain by orders of magnitude, mainly because of the error in the resonance energy for $E_R^{cm} = 330$ keV.

B12. THE ^{32}S$(p, \gamma)^{33}$Cl REACTION

A total of 14 resonances in the region $E_R^{cm} = 75$–2470 keV was considered. Resonances were measured for $E_R^{cm} \geq 409$ keV. The measured strengths have been adopted from Iliadis et al. (1992a) and Aleonard et al. (1976) and normalized to the value $\omega\gamma(E_R^{cm} = 1704 \text{ keV}) = (1.9 \pm 0.2) \times 10^{-1}$ eV, measured in the latter work. The contribution of one threshold state has been taken into account. The spectroscopic factor was adopted from transfer reaction studies (see Table 10). The γ-ray partial width was calculated from the measured lifetime assuming $\Gamma \approx \Gamma_\gamma$. The direct capture contribution has been adopted from Iliadis et al. (1992a). Our total recommended rates agree with the previous results of Iliadis et al. (1992a) at temperatures above $T = 0.15$ GK. However, below this temperature the deviations amount to a factor of 3 because of an improved estimate of $\Gamma_p(E_R^{cm} = 75 \text{ keV})$ in the present work. Our total reaction rates are uncertain by 14% (50%) above (below) $T = 0.15$ GK.

B13. THE ^{35}Cl$(p, \gamma)^{36}$Ar REACTION

A total of 91 resonances in the region $E_R^{cm} = 50$–2828 keV was taken into account. Resonances were measured for $E_R^{cm} \geq 301$ keV. Measured strengths have been adopted from Endt & van der Leun (1978) and from Endt (1998) and references therein. The $\omega\gamma$ values have been normalized by using the results listed in Table 1. Two states near the proton

threshold were taken into account. The spectroscopic factor for the state corresponding to $E_R^{cm} = 50$ keV was adopted from the ^{35}Cl(^{3}He, d)^{36}Ar stripping work of Iliadis et al. (1994). For $E_R^{cm} = 166$ keV, the assignment $J^\pi \leq 4^+$, together with the population of the corresponding level in the ^{32}S(^{6}Li, d)^{36}Ar reaction (Iliadis et al. 1994), yields $J^\pi = 0^+, 1^-, 2^+, 3^-$, and 4^+. The values $J^\pi = 0^+$ and 4^+ can be excluded, since the ^{35}Cl(^{3}He, d)^{36}Ar angular distribution data cannot be described by a pure $l = 2$ transfer (Iliadis et al. 1994). The orbital angular momenta $l = 0 + 2$ (assuming $J^\pi = 2^+$) and $l = 1 + 3$ (assuming $J^\pi = 1^-$ or 3^-), together with the spectroscopic factors given in Iliadis et al. (1994), yield almost identical proton partial widths. The average value is listed in Table 10. The resonance strengths for the threshold states have been estimated with Γ_p and the measured values of Γ_γ/Γ (Ross et al. 1995). The direct capture S-factor was adopted from Iliadis et al. (1994). Our total reaction rates are uncertain by about 20% above $T = 0.2$ GK. For lower temperatures the uncertainties amount to a factor of 2.

B14. THE ^{35}Cl(p, α)^{32}S REACTION

A total of 94 resonances in the region $E_R^{cm} = 50$–2838 keV was taken into account. Resonances were measured for $E_R^{cm} = 849$ keV. Measured strengths have been adopted from Endt & van der Leun (1978) and references therein. The contributions of 18 states close to the proton threshold were taken into account. Only the (p, α) resonance strengths corresponding to the levels at $E_x = 8556$ and 8672 keV are given in Table 10. The strengths have been estimated from the proton partial widths, together with the measured upper limits for Γ_α/Γ (Ross et al. 1995). The proton bombarding energy region of $E_p = 550$–860 keV was not investigated in the ^{35}Cl(^{3}He, d)^{36}Ar studies of Iliadis et al. (1994) and Ross et al. (1995). For this region we adopted for $\omega\gamma_{p\alpha}$ the experimental upper limits quoted in Kuperus, Glaudemans, & Endt (1963). The contribution of low-energy wings of broad resonances has been calculated from measured resonance strengths and widths (Endt & van der Leun 1978). The contribution of subthreshold states has been neglected (see Ross et al. 1995). At $T \geq 3$ GK, our total reaction rates are uncertain by about 30%. At lower temperatures, the uncertainties amount to up to 8 orders of magnitude, mainly because the adopted experimental upper limits of $\omega\gamma_{p\alpha}$ in the energy region $E_p = 550$–860 keV are rather high. Note that the ^{36}Ar level at $E_x = 8887$ keV (Iliadis et al. 1994) corresponding to $E_R^{cm} = 381$ keV was accidentally omitted in Table 36f of Endt (1998).

B15. THE ^{36}Ar(p, γ)^{37}K REACTION

A total of 10 resonances in the region $E_R^{cm} = 312$–2575 keV was considered, with all resonances being measured (Goosman & Kavanagh 1967; Iliadis et al. 1992b; Iliadis et al. 1993b). The measured strengths have been normalized by using the results listed in Table 1. For the level at $E_x = 2285$ keV, corresponding to $E_R^{cm} = 428$ keV, only an upper limit for $\omega\gamma_{p\gamma}$ has been measured (Iliadis et al. 1992b). However, the contribution of this state to the reaction rate is negligible. The direct capture contribution was adopted from Iliadis et al. (1992b). Our recommended total rate deviates from the previous results of Iliadis et al. (1992b) by about 20%, mainly because of the normalization of resonance strengths in the present work according to the values listed in Table 1. In the temperature regions $T < 0.07$ GK, $T = 0.07$–1.0 GK and $T > 1.0$ GK our total reaction rates are uncertain by 35%, 15% and 8%, respectively.

B16. THE ^{35}K(p, γ)^{36}Ca REACTION

Excited states in the compound nucleus ^{36}Ca have not been observed. The contribution of only one level, corresponding to $E_R^{cm} = 700$ keV, was taken into account. The excitation energy was estimated previously by using Coulomb displacement energy calculations (Herndl et al. 1995), and the result was adopted in the present work. The shell model spectroscopic factor has been adopted from Herndl et al. (1995). In the latter work the γ-ray partial width has also been calculated with the shell model. However, here we use instead the measured lifetime of the ^{36}Si mirror state. It is shown in Iliadis et al. (1999) that this procedure yields reliable results on average within a factor of about 2. The direct capture contribution was adopted from Herndl et al. (1995). Our recommended total rate agrees with the results of Herndl et al. (1995) at temperatures $T \leq 0.15$ GK for which the direct capture process is dominant. However, for higher temperatures the present and previous rates deviate by a factor of 10, mainly because we use the experimental lifetime of the mirror state instead of shell model results. The total recommended rates are uncertain by orders of magnitude due to uncertainties in the excitation energy of the first excited state in ^{36}Ca.

B17. THE ^{40}Ca(p, γ)^{41}Sc REACTION

A total of eight resonances in the region $E_R^{cm} = 631$–1887 keV was considered and all resonances have been measured (Endt 1990 and references therein). The measured strengths have been normalized by using the results listed in Table 1. Note that the strength of the lowest-lying resonance at $E_R^{cm} = 631$ keV quoted in Endt (1990) is erroneous (P. M. Endt 1998, private communication). The correct value $\omega\gamma_{p\gamma} = (1.8 \pm 0.2) \times 10^{-3}$ eV has been used in the present work. The levels at $E_x = 2096$ and 2415 keV have not been observed as resonances at $E_R^{cm} = 1011$ and 1330 keV, respectively. The resonance parameters were estimated by using measured proton spectroscopic factors (Endt & van der Leun 1978) and experimental lifetimes of ^{41}Ca mirror states (Endt 1990). The reaction rate contribution of these two states is found to be negligible. The direct capture contribution has been estimated in the present work. Our result is smaller by a factor of ≈ 3 compared with the direct capture S-factor quoted in Wiescher & Görres (1989), presumably due to numerical instabilities in the calculations of their work. Our recommended total rates deviate at $T \geq 0.2$ GK from the results of Wiescher & Görres (1989) by about 30%, mainly because of the normalization of resonance strengths in the present work according to the values listed in Table 1. At lower temperatures the deviations amount to a factor of 3 due to differences in the adopted direct capture S-factor. Our total reaction rates are uncertain by 13% (35%) above (below) $T = 0.2$ GK.

REFERENCES

Aleonard, M. M., Hubert, P., Sarger, L., & Mennrath, P. 1976, Nucl. Phys. A, 257, 490
Anderson, M. R., Kennett, S. R., Mitchell, L. W., & Sargood, D. G. 1980, Nucl. Phys. A, 349, 154
Angulo, C., et al. 1999, Nucl. Phys. A, 656, 3
Audi, G., & Wapstra, A. H. 1995, Nucl. Phys. A, 595, 409
Bateman, N., et al. 2001, Phys. Rev. C, in press
Benenson, W., Mueller, D., Kashy, E., Nann, H., & Robinson, L. W. 1977, Phys. Rev. C, 15, 1187
Blatt, J. M., & Weisskopf, V. F. 1952, Theoretical Nuclear Physics (New York: Wiley)
Buchmann, L., Becker, H. W., Kettner, K. U., Kieser, W. E., Schmalbrock, P., & Rolfs, C. 1980, Z. Phys. A, 296, 273
Burbidge, E. M., Burbidge, G. R., Fowler, W. A., & Hoyle, F. 1957, Rev. Mod. Phys., 29, 547
Caggiano, J., et al. 2001, in preparation
Caughlan, G. R., & Fowler, W. A. 1988, At. Data Nucl. Data Tables, 40, 283
Champagne, A. E., Brown, B. A., & Sherr, R. 1993, Nucl. Phys. A, 556, 123
Champagne, A. E., Cella, C. H., Kouzes, R. T., Lowry, M. M., Magnus, P. V., Smith, M. S., & Mao, Z. Q. 1988, Nucl. Phys. A, 487, 433
Champagne, A. E., Pitt, M. L., Zhang, P. H., Lee, L. L., & Levine, M. J. 1986, Nucl. Phys. A, 459, 239
Chronidou, C., Spyrou, K., Harissopulos, S., Kossionides, S., & Paradellis, T. 1999, Eur. Phys. J. A, 6, 303
Dykoski, W. W., & Dehnhard, D. 1976, Phys. Rev. C, 13, 80
Elbakr, S. A., Glavina, C., Dawson, W. K., Gupta, V. K., McDonald, W. J., & Neilson, G. C. 1972, Can. J. Phys., 50, 674
El Eid, M. F., & Champagne, A. E. 1995, ApJ, 451, 298
Endt, P. M. 1990, Nucl. Phys. A, 521, 1
———. 1998, Nucl. Phys. A, 633, 1
Endt, P. M., & Rolfs, C. 1987, Nucl. Phys. A, 467, 261
Endt, P. M., & van der Leun, C. 1978, Nucl. Phys. A, 310, 1
Fowler, W. A., Caughlan, G. R., & Zimmerman, B. A. 1967, ARA&A, 5, 525
Goosman, D. R., & Kavanagh, R. W. 1967, Phys. Rev. C, 161, 1156
Gove, H. E. 1959, in Nuclear Reactions I, ed. P. M. Endt & M. Demeur (New York: North Holland), 259
Hale, S. E., et al. 2001, in preparation
Hauser, W., & Feshbach, H. 1952, Phys. Rev., 87, 366
Herndl, H., Fantini, M., Iliadis, C., Endt, P. M., & Oberhummer, H. 1998, Phys. Rev. C, 58, 1798
Herndl, H., Görres, J., Wiescher, M., Brown, B. A., & Van Wormer, L. 1995, Phys. Rev. C, 52, 1078
Hoffman, R. D., Woosley, S. E., Weaver, T. A., Rauscher, T., & Thielemann, F.-K. 1999, ApJ, 521, 735
Iliadis, C. 1997, Nucl. Phys. A, 618, 166
Iliadis, C., Buchmann, L., Endt, P. M., Herndl, H., & Wiescher, M. 1996, Phys. Rev. C, 53, 475
Iliadis, C., Endt, P. M., Prantzos, N., & Thompson, W. J. 1999, ApJ, 524, 434
Iliadis, C., Giesen, U., Görres, J., Wiescher, M., Graff, S. M., Azuma, R. E., & Barnes, C. A. 1992a, Nucl. Phys. A, 539, 97
Iliadis, C., et al. 1994, Nucl. Phys. A, 571, 132
Iliadis, C., et al. 1993a, Nucl. Phys. A, 559, 83
Iliadis, C., Höhne, J., Käppeler, F., Meissner, J., Trautvetter, H. P., & Wiescher, M. 1993b, Phys. Rev. C, 48, R1479
Iliadis, C., Ross, J. G., Görres, J., Wiescher, M., Graff, S. M., & Azuma, R. E. 1992b, Phys. Rev. C, 45, 2989
Iliadis, C., et al. 1990, Nucl. Phys. A, 512, 509
Inglima, G., Caracciolo, R., Cuzzocrea, P., Perillo, E., Sandoli, M., & Spadaccini, G. 1975, Nuovo Cimento, 26, 211
Kalifa, J., Vernotte, J., Deschamps, Y., Pougheon, F., Rotbard, G., Vergnes, M., & Wildenthal, B. H. 1978, Phys. Rev. C, 17, 1961
Kubono, S., et al. 1992, Nucl. Phys. A, 537, 153
Kuperus, J., Glaudemans, P. W. M., & Endt, P. M. 1963, Physica, 29, 1281
Lane, A. M., & Thomas, R. G. 1958, Rev. Mod. Phys., 30, 257
Mackh, H., Wagner, G. J., Dehnhard, D., & Ohnuma, H. 1973, Nucl. Phys. A, 202, 497
Mermaz, M. C., Whitten, C. A., Champlin, J. W., Howard, A. J., & Bromley, D. A. 1971, Phys. Rev. C, 4, 1778
Mohr, P., Oberhummer, H., Gyürky, G., Somorjai, E., Kiss, A. Z., & Borbely-Kiss, I. 1999, Phys. Rev. C, 59, 1790
Neogy, P., Middleton, R., & Scholz, W. 1972, Phys. Rev. C, 6, 885
Paine, B. M., & Sargood, D. G. 1979, Nucl. Phys. A, 331, 389
Powell, D. C., Iliadis, C., Champagne, A. E., Grossmann, C. A., Hale, S. E., Hansper, V. Y., & McLean, L. K. 1999, Nucl. Phys. A, 660, 349
Powell, D. C., Iliadis, C., Champagne, A. E., Hale, S. E., Hansper, V. Y., Surman, R. A., & Veal, K. D. 1998, Nucl. Phys. A, 644, 263
Rauscher, T., & Thielemann, F.-K. 2000, At. Data Nucl. Data Tables, 75, 1
Rauscher, T., Thielemann, F.-K., & Kratz, K.-L. 1997, Phys. Rev. C, 56, 1613
Rolfs, C. 1973, Nucl. Phys. A, 217, 29
Rolfs, C., Shapiro, M. H., & Winkler, H. 1975, Nucl. Phys. A, 241, 460
Ross, J. G., et al. 1995, Phys. Rev. C, 52, 1681
Sargood, D. G. 1982, Phys. Rep., 93, 61
Schatz, H., et al. 1997, Phys. Rev. Lett., 79, 3845
Schiffer, J. P. 1963, Nucl. Phys., 46, 246
Seuthe, S., et al. 1990, Nucl. Phys. A, 514, 471
Thompson, W. J., & Iliadis, C. 1999, Nucl. Phys. A, 647, 259
Timmermann, R., Becker, H. W., Rolfs, C., Schröder, U., & Trautvetter, H. P. 1988, Nucl. Phys. A, 477, 105
Trautvetter, H.-P., & Rolfs, C. 1975, Nucl. Phys. A, 242, 519
Van Wormer, L., Görres, J., Iliadis, C., & Wiescher, M. 1994, ApJ, 432, 326
Vernotte, J., Khendriche, A., Berrier-Ronsin, G., Grafeuille, S., Kalifa, J., Rotbard, G., Tamisier, R., & Wildenthal, B. H. 1990, Phys. Rev. C, 41, 1956
Vogelaar, B., et al. 2001, in preparation
Wallace, R. K., & Woosley, S. E. 1981, ApJS, 45, 389
Wiescher, M., et al. 1980, Nucl. Phys. A, 349, 165
Wiescher, M., & Görres, J. 1988, Z. Phys. A, 329, 121
———. 1989, ApJ, 346, 1041
Wiescher, M., Görres, J., Thielemann, F.-K., & Ritter, H. 1986, A&A, 160, 56
Yokata, H., Fujioka, K., Ichimaru, K., Mihara, Y., & Chiba, R. 1982, Nucl. Phys. A, 383, 298